

# Multimode rotationally symmetric bosonic codes from group-theoretic construction

Rabsan Galib Ahmed,<sup>1,2</sup> Adithi Udupa,<sup>2</sup> and Giulia Ferrini<sup>2</sup>

<sup>1</sup>*Department of Physical Sciences, Indian Institute of Science Education and Research Mohali, Punjab 140306, India*

<sup>2</sup>*Department of Microtechnology and Nanoscience, Chalmers University of Technology, Göteborg SE-412 96, Sweden*

We introduce a new family of multi-mode, rotationally symmetric bosonic codes inspired by the group-theoretic framework of [Phys. Rev. Lett. 133, 240603 (2024)]. Such a construction inverts the traditional paradigm of code design by identifying codes from the requirement that a group of chosen logical gates should be implemented by means of physically simple logical operations, such as linear optics. Leveraging previously unexplored degrees of freedom within this framework, our construction results in codes that display rotational symmetry across multiple modes, while enabling linear-optics implementation of the full Pauli group. These codes exhibit improved protection against dephasing noise, outperforming both single-mode analogues and earlier multi-mode constructions. Notably, they allow exact correction of correlated dephasing and support qudit encoding in arbitrary dimensions. We analytically construct and numerically benchmark two-mode binomial codes instances, and demonstrate that, unlike single-mode rotationally symmetric bosonic codes, these exhibit no trade-off between protection against dephasing and photon loss.

Bosonic codes allow for encoding the logical quantum information of a qubit in the (infinitely) many levels of a quantum harmonic oscillator, providing enhanced robustness to noise and holding promise for building scalable architecture of fault-tolerant quantum computers [1]. In the recent years, they have been used for enhancing the life time of quantum information beyond one of the elementary experimental components, i.e. to reach the so-called "break-even" regime [2, 3]. Furthermore, using bosonic codes as the physical qubits allows for reducing the size of discrete-variable codes concatenated to the bosonic code, such as for the surface and LDPC codes, while keeping the same performance [4–11]. This in turns induces an increased algorithmic performance as compared to the use of standard qubits [12].

One way to understand the performance of bosonic codes is in terms of their symmetries. For instance,  $N$ -order rotationally symmetric bosonic (RSB) codes [13] have a specific structure of the codewords in Fock space, where only Fock states with multiples of  $N$  are allowed. This structure implies that RSB codes allow for detecting the loss or gain of up to  $N - 1$  photons at the same time, while also tolerating phase errors of magnitude up to  $\pi/N$ . While such codes have the potential to break even in relevant parameter regimes, finding new bosonic codes with better performance is essential to further reduce the overhead of physical qubits needed in practical implementations of concatenated codes. Furthermore, the implementation of relevant gates such as the logical  $X$ -gate on such codes is complicated, and requires the use of auxiliary qubits. Therefore it is essential to design new bosonic codes with good quantum error correcting (QEC) properties, and at the same time with easily implementable sets of logical gates.

While usual approaches to the design of QEC codes consist of first introducing a code, and then finding the operations that implement the logical gates on that code, Ref. [14] takes an opposite approach. It provides a group-theoretic construction where one first selects a chosen group of logical gates, e.g. the Pauli group, to be implemented by simple physical operations, e.g. linear optics, and then a corresponding code is identified, where the desired logical gates are implemented by means of the chosen simple physical operations.

In this work, we exploit some previously unexplored free-

dom in the construction of Ref. [14], to introduce a new family of multi-mode bosonic codes with rotational symmetry, that we therefore call multi-mode RSB codes. These codes retain the advantage of the ones in Ref. [14], as their logical Pauli operations remain implementable via linear optics, while also offering enhanced performance against dephasing errors compared with the corresponding instances in Ref. [14]. Furthermore, this multimode extension also allows us to encode qudits of arbitrary dimension. We perform a detailed analytical and numerical analysis of the performance of such codes for the case of the two-mode binomial code, which can be thought as the two-mode generalization of the binomial code [13, 15]. We provide analytical and numerical evidence showing that, in contrast to the single-mode version of this code, which displays a trade-off between the capability of detecting loss or dephasing errors at increasing order of the discrete rotational symmetry  $N$  [13], our two-mode binomial code offers a simultaneous improvement of the error detection capability, yielding an overall improvement in the error correction performance over the single-mode case. Furthermore, we show that any two-mode RSB code in our family of codes offers perfect protection against correlated dephasing.

*Preliminaries* — The essential idea behind the group-theoretic encoding of Ref. [14] is to find a subspace of the Hilbert space of a given physical system, called the *codespace*, that is isomorphic to the logical space, such that a group of logical operations are *easily implementable*. It takes as inputs: a group,  $G$ , and its representations,  $\lambda$  and  $\pi$ , on the logical and physical Hilbert space respectively, where  $\pi$  is constructed using a set of physical operations that we define as easily implementable. The output of this construction is a family of codespaces, from which the codespace performing optimally against relevant noise channels can be chosen. As an application, a two-mode bosonic code has been proposed in Ref. [14], when  $G$  is chosen to be isomorphic to the Pauli group,  $\langle X, Z \rangle$  and the physical representation,  $\pi$ , is constructed with passive linear operations on two modes. The resulting *Pauli code* has been shown to perform better than the dual-rail code against the pure loss channel in the two modes. However, the construction itself offers more freedom in choosing  $G$  and  $\pi$  than it was explored in Ref. [14].

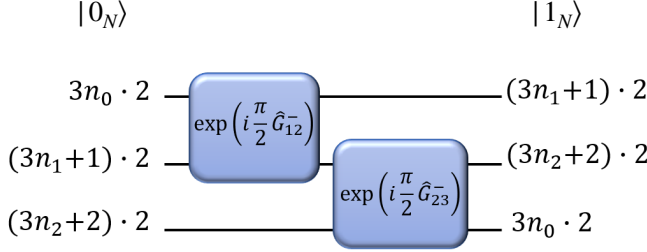


FIG. 1: Application of the logical  $X$  gate on a qutrit ( $d = 3$ ) encoded in a three mode rotation-symmetric bosonic code of order  $N = 2$ . Each of the lines indicates a single bosonic mode.

*Multimode rotation symmetric bosonic codes* — We start by showing that an extended construction allows us for encoding a qudit, having a  $d$ -dimensional Hilbert space, in a new family of multimode RSB codes, hosted by  $d$  bosonic modes. The Pauli group for a qudit is generated by  $X$  and  $Z$ . In the computational basis, their actions are given by  $X|k\rangle = |k \oplus 1\rangle$ ,  $Z|k\rangle = \omega_d^k|k\rangle$ , where  $\omega_d = e^{2\pi i/d}$ . Inspired by, but distinctly from, the construction of Ref. [14], we choose the group  $G$  to be  $G = \langle g, h | h^{2N} = e \rangle$  for an even  $N$  and the representations  $\lambda(g) = X$ ,  $\lambda(h) = Z$  and [16]

$$\pi(g) = \hat{U}_{BS} \left( \prod_{i=1}^{d-1} e^{-i\frac{\pi}{2} \hat{G}_{i,i+1}^-} \right)^\dagger \hat{U}_{BS}^\dagger, \quad (1)$$

$$\pi(h) = \hat{U}_{BS} e^{i\frac{2\pi}{N} \hat{a}_1^\dagger \hat{a}_1} \hat{U}_{BS}^\dagger. \quad (2)$$

Here  $\hat{U}_{BS} := \exp \left\{ i \sum_{j,k=1; j < k}^d \left( \theta_{jk}^- \hat{G}_{jk}^- + \theta_{jk}^+ \hat{G}_{jk}^+ \right) \right\}$  is a general passive linear operation generated by beam-splitters on all pairs of modes  $(j, k)$ , with  $\hat{G}_{jk}^+ = \hat{a}_j^\dagger \hat{a}_k + \hat{a}_k^\dagger \hat{a}_j$  and  $\hat{G}_{jk}^- = i(\hat{a}_j^\dagger \hat{a}_k - \hat{a}_k^\dagger \hat{a}_j)$  and  $\theta^\pm$ 's some real numbers parametrising  $\hat{U}_{BS}$ . Crucially, this mode mixing operation, absent in the construction of Ref. [14], endows the code with additional freedom in the choice of the encoding modes, which, as we will see, will result in an enhancement of the code performance. A beam-splitter for encoding a multimode bosonic code was considered with NOON states in Ref.[17]. We find that the  $d$ -dimensional subspace of  $d$  physical modes, where Eqs.(1) and (2) operate as logical  $X$  and  $Z$  respectively, is spanned by the the computational codewords

$$|k_N\rangle = \hat{U}_{BS} \sum_{\{n_i\}=0}^{\infty} f_{n_0 \dots n_{d-1}} \bigotimes_{j=k}^{k \oplus (d-1)} |(dn_j + j)N\rangle, \quad (3)$$

where  $\oplus$  is addition modulo  $d$ , the indexes  $\{n_i\}$  run between 0 and  $\infty$ , and  $f_{n_0 \dots n_{d-1}}$ 's are coefficients that can be chosen freely, provided they satisfy normalisation. The derivation is given in Appendix A. We also assume that if the upper limit on the product sign,  $\bigotimes$ , is less than the lower limit, then the index  $j$  runs a period through  $\mathbb{Z}/d\mathbb{Z}$ . For exam-

ple, when  $k = 1, d = 3$ ,  $j$  runs through 1, 2, 0; hence the product state is  $| (3n_1 + 1)N \rangle \otimes | (3n_2 + 2)N \rangle \otimes | 3n_0 N \rangle$ . In each of the modes, we have an order- $N$  rotation symmetry, as can be verified by applying the order- $N$  rotation symmetry operator  $\hat{R}_N^{(k)} = e^{i2\pi \hat{n}_k/N}$  to the codeword, where  $\hat{n}_k = \hat{U}_{BS} \hat{a}_k^\dagger \hat{a}_k \hat{U}_{BS}^\dagger$ . As an illustration, the action of the logical operator  $X$  stemming from Eq.(1) on a qutrit ( $d = 3$ ) encoded in a three mode rotation-symmetric bosonic code of order  $N = 2$  is illustrated in Fig.1. Note the similarity of the Fock-space structure with the case of single-mode RSB qudits, as defined in Appendix F of Ref.[18]. Distinct multimode bosonic codes with rotational symmetry were introduced from homological rotor codes in Ref.[19]. Other codes exhibiting rotational symmetry have been studied in the context of single-photon implementations of GKP states [20].

*Two-mode instance and comparison with previous codes*— As a special case of the multimode encoding of a qudit, we focus on the case when  $d = 2$ : encoding a qubit in two bosonic modes. The most general codewords are explicitly given by

$$|0_N\rangle = \hat{U}_{BS} \sum_{m,n} f_{mn} |2mN, (2n+1)N\rangle \quad (4)$$

$$|1_N\rangle = \hat{U}_{BS} \sum_{m,n} f_{mn} |(2n+1)N, 2mN\rangle \quad (5)$$

with  $\hat{U}_{BS} = \exp \left[ i\delta(\hat{G}_{12}^+ \sin \phi + \hat{G}_{12}^- \cos \phi) \right]$ . By construction, the logical bit-flip gate,  $X$ , is implemented in these codewords by  $\hat{U}_{BS} e^{-i\pi \hat{G}_{12}^-/2} \hat{U}_{BS}^\dagger$ , here corresponding to a SWAP gate, and the logical phase-flip gate,  $Z$ , is implemented by  $\hat{U}_{BS} e^{i\pi \hat{a}_1^\dagger \hat{a}_1/N} \hat{U}_{BS}^\dagger$ . If we disregard the beam-splitter  $\hat{U}_{BS}$ , choosing the  $f_{m,n} \propto \frac{e^{-2|\alpha|^2}}{\sqrt{(2mN)!(2n+1)N!}} \alpha^{2mN} \alpha^{(2n+1)N}$  yields the concatenation of a cat code with a dual-rail code [21] (reminiscent of the cat repetition code [22]). This is distinct from the pair cat-codes found in [23], where the codewords are eigenstate of the difference between the number operators of the two modes. The choice  $f_{m,n} = 1 \forall m,n$  yields instead the concatenated dual-rail ideal number-phase code [13] (reminiscent of the repetition number-phase code). However, we choose here  $f_{mn} = \frac{1}{\sqrt{2}}$  when  $(m,n) = (0,0)$  and  $(1,0)$ , and,  $f_{mn} = 0$  for any other  $(m,n)$ . This yields the concatenated dual-rail binomial code ( $K = 2$ )

$$|0_N\rangle = \hat{U}_{BS}(\delta, \phi) \frac{1}{\sqrt{2}} (|0\rangle + |2N\rangle) \otimes |N\rangle \quad (6)$$

$$|1_N\rangle = \hat{U}_{BS}(\delta, \phi) |N\rangle \otimes \frac{1}{\sqrt{2}} (|0\rangle + |2N\rangle), \quad (7)$$

with  $N$  being the order of rotation symmetry, and the encoding-dependent angles  $(\delta, \phi)$ , here explicated, parameterising the beam-splitting operator  $\hat{U}_{BS}$ . We refer to these codes as the *two-mode  $K = 2$  codes*. These codewords are similar, although distinct, to the two-qubit binomial encoded Bell state of Ref.[24] [25]. As compared to concatenation with repetition-code, the relatively uniform distribution of the bosonic excitations across the two-modes of our codes holds

potential for increased QEC performance, as we now address.

*Performance of two-mode binomial code under losses and dephasing channels* — We now analyse the performance of the simplest instances of this family of codewords mentioned above, corresponding to the binomial case Eqs.(6) and (7), for the cases of  $N = 2$  and  $N = 4$ .

We compare the performance of these new codes with the previous single-mode binomial code, as well as with the two-mode CLY code of Ref.[26], against the pure loss, pure dephasing and finally the combined loss-dephasing channels. Note that the CLY is generally not an instantiation of the family of codes proposed here. In the most general case of the combined channel, the Kraus representation is given by

$$\mathcal{N}_L \circ \mathcal{N}_D \sim \{\hat{L}_p^{(1)} \hat{L}_q^{(2)} \hat{D}_r^{(1)} \hat{D}_s^{(2)} : p, q, r, s \in \mathbb{N}_0\}, \quad (8)$$

where the Kraus operators for the loss and dephasing channel in each mode,  $i = 1, 2$ , are respectively given by

$$\hat{L}_p^{(i)} = \sqrt{\frac{(1 - e^{-\kappa_i t})^p}{p!}} e^{-\frac{1}{2}\kappa_i t} \hat{a}_i^\dagger \hat{a}_i \hat{a}_i^p, \quad (9)$$

$$\hat{D}_r^{(i)} = \sqrt{\frac{(\gamma_i t)^r}{r!}} e^{-\frac{1}{2}\gamma_i t} (\hat{a}_i^\dagger \hat{a}_i)^2 (\hat{a}_i^\dagger \hat{a}_i)^r. \quad (10)$$

The loss and dephasing strength of the channels are respectively quantified by the parameters  $\kappa_i t$  and  $\gamma_i t$  in each mode. In the comparison, we also consider the "break-even threshold", which is defined here as the average fidelity of a logical qubit that is constructed with the ground state ( $|0\rangle$ ) and the first excited state ( $|1\rangle$ ) of a harmonic oscillator, called the *trivial encoding*, subjected to relevant noise channels but without a recovery operation [2, 3].

Let us start with analysing the performance under a pure dephasing channel. We observe that the performance of the two-mode codes depends in this case on the encoding angles  $(\delta, \phi)$ . We find with both numerical and analytical analysis (as we will detail further) that the optimal performance against Gaussian dephasing noise is achieved for  $\delta = \pi/4, 3\pi/4, \phi = \pi/(2N)$ . For this choice of angles, the performance of the two-mode binomial code is significantly better than for the case of the single-mode binomial code, see Figure 2 a).

For single-mode RSB codes, there is a trade-off between the performance of the codes against loss and dephasing noise [13]: the performance against losses increases at increasing  $N$ , while for dephasing it decreases at increasing  $N$ , up to an optimal value of  $N$ , after which the performance decreases with  $N$  for both noise channels. Strikingly, up to this optimum value of  $N$ , we observe instead a significant improvement in performance under the dephasing noise channel of our two-mode binomial code for the optimal choice of the encoding angles  $(\delta, \phi)$ , which results in a simultaneous improvement of the performance with increasing  $N$  up to an optimal value of  $N$ , see Figure 2 a) and b). The performance analysis for each of the noise models studied has been carried out by numerically solving the semi-definite programming of finding the optimal recovery map [27]. In Fig. 2 c) we present the results for the combined dephasing-loss channel.

To correct the effect of the noise channel (loss or dephasing or both) up to the first order in the noise strength for an arbitrary logical state prepared in the codewords Eqs.(6) and (7), we propose a two-mode extension of the recovery map outlined for the simplest single-mode bosonic codes [2, 15]: a modular number measurement (a generalised number-parity measurement) indicates the error-syndrome, and corresponding unitary operators are applied. In Appendix B, we provide the first order expansion of the noise operators for loss and dephasing. We observe that the codewords for  $K = 2, N = 2$  satisfy the Knill-Laflamme conditions exactly for the loss channel up to the first order in the loss rate, allowing us to find the corresponding recovery map. This is also the case for  $K = 2, N = 4$ , where additionally, for the optimal choice of angles  $\delta = \pi/4, 3\pi/4$ , the Knill-Laflamme conditions are also satisfied for the case of dephasing, up to the first-order in dephasing rate. The details of the recovery map based on modular number measurement for the case of  $K = 2, N = 2$  and  $K = 2, N = 4$  are provided in Appendices C and D. This finding for dephasing corroborates the optimal encoding angles that we found numerically and expected from the analysis in Appendix E1.

*Understanding the code performance against dephasing in terms of Knill-Laflamme conditions and codewords distinguishability* — For dephasing noise, we show in Appendix E1 that, for optimal angles  $\delta = \pi/4, 3\pi/4, \phi = \pi/(2N)$ , as  $N$  approaches infinity, the KL conditions get closer to being exactly satisfied not only at first order in the dephasing parameter, but for any value of dephasing. This validates the performance increase at increasing  $N$  observed numerically. The increased performance against dephasing for the optimal choice of encoding angles as compared to the case of single-mode RSB codes can be further analysed in terms of the codewords distinguishability under phase measurements. In a previous study [28], we have found that the performance of the single-mode rotation symmetric codes for the Knill teleportation based error-correcting (telecorrection) circuit against a purely dephasing noise is upper bounded by a monotonically increasing function of the distinguishability between the dual codewords,  $|\pm_N\rangle$ . In order to assess this distinguishability, one can employ the *canonical phase measurement* [13, 29]. What we essentially found in [28] is that, as long as the probability distributions of the outcomes of the phase measurements for the codewords,  $|+_N\rangle$  and  $|-_N\rangle$ , do not significantly overlap under the evolution of a dephasing noise, it is possible to recover the logical state faithfully on average. Here we extend this understanding to the case of two-mode rotation-symmetric codes by analysing the phase measurements on the two modes. Unlike the case of single-mode codes, where the phase measurement outcomes lie in a circle,  $[0, 2\pi) \cong S^1$ , those in the case of two-mode codes lie in a torus,  $S^1 \times S^1$ . Therefore, in contrast to the single-mode codes where the distributions inevitably overlap in the circle,  $S^1$ , for the two-mode codes, with different choices of the encoding angles,  $\delta, \phi$ , the distributions can be made to avoid each other on the torus,  $S^1 \times S^1$  (see Appendix E2 for more details). We emphasize that, despite these arguments are based on distinguishability with respect to phase measurements, for correct-

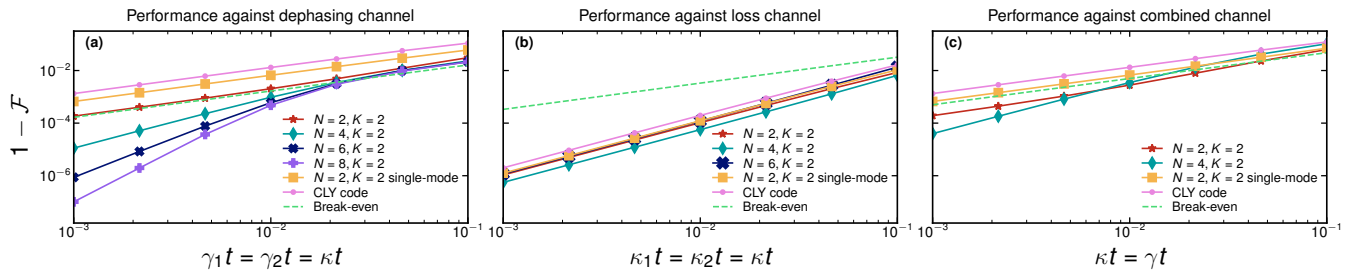


FIG. 2: Performance of the simple instances in Eqs.(6) and (7) of the two-mode rotation symmetric code constructed in this paper against (a) the dephasing channel with equal rates in both the modes,  $\gamma_1 = \gamma_2 = \gamma$ , (b) the loss channel with  $\kappa_1 = \kappa_2 = \kappa$ , and (c) a combination of both of these noisy channels with equal strengths in both the modes and with  $\gamma = \kappa$ . In all the three cases, we have chosen the optimal values of the beam-splitter angles  $(\delta, \phi)$  and we note that under the loss channel, the performance is independent of this choice. We also compare against the  $N = 2, K = 2$  single-mode binomial code, the two-mode CLY code, as well as to the break-even. For dephasing, we also report the performance for  $K = 2, N = 6$  and  $K = 2, N = 8$ , corroborating the performance increase at increasing  $N$ . We note that under the dephasing channel the evolution is restricted to a smaller subspace than the full Hilbert space that is required to describe a general evolution of the codewords. This allows us to go to higher values of  $N$  to evaluate the performance of the code under the purely dephasing channel. We note that the optimum value of  $N$  under the loss channel displayed in panel (b) is around  $N = 4$ , which is similar to the corresponding case of the single-mode code [13]. Our two-mode codes show comparable performance to the corresponding  $N$ -order single-mode code under the loss channel, while they enhance the performance quite significantly against the dephasing channel (panel (a)).

ing the dephasing noise to the leading orders in case of the smallest instances of the two-mode code we use the modular number measurement to reveal the error syndrome as described in Appendices C and D.

We have also verified that the increase in performance of the two-mode binomial case as compared to the single-mode case for the optimal choice of the encoding angles is robust even in the case of more sophisticated instances of dephasing channels, such as non-Markovian dephasing induced by random telegraph noise [28, 30–34], see Appendix F.

*Performance of two-mode RSB under correlated dephasing* — Correlated dephasing can arise e.g. as a result of the usually strong dephasing of flux tunable couplers such as SNAIL-based modes [35, 36], noise which is picked up by the coupled bosonic modes. This can be modelled through a stochastic interaction Hamiltonian,  $\hat{H}(t) = \nu c(t)(\hat{a}_1^\dagger \hat{a}_1 + \hat{a}_2^\dagger \hat{a}_2)$ , where  $c(t)$  is a stochastic variable. The effective noise channel is given in this case by

$$\mathcal{N}(\hat{\rho}) = \int_{-\infty}^{\infty} d\phi p_t(\phi) e^{i\phi(\hat{n}_1 + \hat{n}_2)} \hat{\rho} e^{-i\phi(\hat{n}_1 + \hat{n}_2)}. \quad (11)$$

Here we show that for any choice of two-mode RSB code in Eqs.(4) and (5), the quantum circuit in Fig. 3 corrects exactly any such arbitrary correlated dephasing noise of the form in Eq.(11). Here, modes 1, 2 and 3, 4 encode the control and the target qubits, respectively. The first controlled- $X$  ( $CX$ ) gate in Fig. 3 between two qubits encoded in order- $N$  (control qubit) and order- $M$  (target qubit) two-mode RSB code is implemented by the unitary  $CX_{NL} = \exp\left(i\frac{\pi}{2N}\hat{n}_1 \otimes \hat{G}_{34}^-\right)$ . The second control unitary in Fig. 3 is given by  $\exp\left(i\frac{\pi}{2N}\hat{n}_3 \otimes \hat{G}_{12}^-\right)$ . In Appendix G, we analyti-

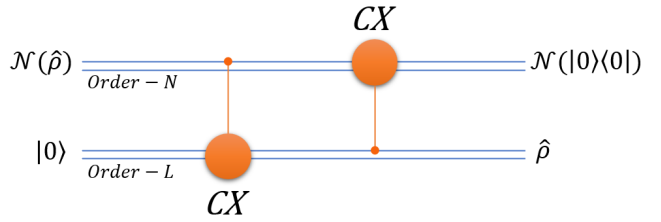


FIG. 3: Exact error-correcting circuit for correlated stochastic dephasing noise.

cally derive the action of this circuit and establish the exact correction of such a correlated noise.

*Application of other gates* — The group of logical operators that we have chosen to be implemented through the *easy* operations, namely the passive linear operations, is the Pauli group. However, that is not enough to achieve universal quantum computation. For that purpose we additionally give a prescription for the application of the Hadamard gate ( $H$ ), the phase gate ( $S$ ), the  $T$ -gate ( $T$ ) and the two-qubit control- $Z$  gate ( $CZ$ ). Similarly to the case of the Pauli code discussed in Ref. [14], for our family of codes, for general even  $N$ , the  $S$  and the  $CZ$  gate can be applied using the non-linear interactions of a microwave resonator [13]. Explicitly, for an even- $N$  two-mode code, we have  $\hat{S}_N = \exp(i\frac{\pi}{2N^2}\hat{n}_1^2)$ , implementable using the self-Kerr interaction. The  $CZ$  gate between two qubits encoded in order- $N$  and order- $M$  can be applied similarly using the cross-Kerr interaction between two microwave resonator:  $CZ_{NM} = \exp(i\frac{\pi}{NM}\hat{n}_1 \otimes \hat{n}_3)$  [13], where the interaction happens between the first mode of each of the two encoded bosonic qubits. The  $H$  and  $T$  gates can

be implemented using teleported gates, similar to what was proposed in [13]. For this purpose, an auxiliary qubit, encoded in two modes, is initially prepared in the states,  $|+_N\rangle = \frac{1}{\sqrt{2}}(|0_N\rangle + |1_N\rangle)$  and  $|T_N\rangle = \frac{1}{\sqrt{2}}(|0_N\rangle + e^{i\pi/4}|1_N\rangle)$  respectively, followed by a coupling to the two-mode data qubit using a  $CZ$  gate and a phase measurement on the data qubit. The resultant state of the auxiliary qubit contains the desired action of the gates up to an action of a logical  $X$ . The circuits are included in Appendix H.

*Conclusive remarks and open questions* — We have introduced a new family of multimode bosonic codes, which extends the rotationally symmetric bosonic codes introduced in Ref. [13] to the multimode, multidimensional case, inspired by the group theoretic construction introduced in Ref. [14]. An analysis of the two-mode binomial instance reveals increased performance as compared to the single-mode case, in particular against dephasing noise, where the trade-off between resilience towards dephasing and loss errors at increasing discrete symmetry order  $N$  that affects the single-mode RSB codes (up to the optimum  $N$ ) is resolved. This increase in performance achieved by increasing the number of modes in the codes echoes similar results found for translationally symmetric bosonic codes [37, 38], but was not found before for RSB codes, to the best of our knowledge.

Several directions for further research arise from our work. For example, the very general codewords presented in Eq.(3) yield a family of codes, with vast space for numerical optimization of the parameters, given a specific noise model, such

as qudit dimensionality, order of rotational symmetry, and coefficients of the superposition. Furthermore, for the codes studied in this work we have chosen the Pauli group as the group to be implemented covariantly; it is an interesting question to ask what codes would stem by selecting other representations of the Clifford group or of groups homomorphically equivalent to it, than those considered in Ref. [14]. Finally, it is interesting to consider the case where physically implementable operations are not constrained to passive linear optical operations, but correspond instead to more sophisticated operations, such as those implementable with superconducting circuits [39, 40].

*Acknowledgment* — We acknowledge useful discussions with Tahereh Abad, Victor Albert, Kunal Dhanraj Helambe, Axel Eriksson, Yvonne Gao, Simone Gasparinetti, Mats Granath, Trond Haug, Maryam Khanahmadi, Martin Jirelow, Anthony Leverrier, Anja Metelmann, Lukas Splitthof, Peter van Loock, and Suocheng Zhao. G.F. acknowledges funding from the European Union’s Horizon Europe Framework Programme (EIC Pathfinder Challenge project Veriqub) under Grant Agreement No. 101114899, the Olle Engkvist Foundation, and the Swedish Research Council through the project grant VR DAIQUIRI. G.F. and A.U. acknowledge support from the Knut and Alice Wallenberg Foundation through the Wallenberg Center for Quantum Technology (WACQT). G.F., A.U. and R. G. A. acknowledge funding from Chalmers Area of Advance Nano, as well as resources at the Chalmers Centre for Computational Science and Engineering (C3SE).

---

[1] V. V. Albert, in *Quantum Fluids of Light and Matter* (IOS Press, 2025) pp. 79–107.

[2] Z. Ni, S. Li, X. Deng, Y. Cai, L. Zhang, W. Wang, Z.-B. Yang, H. Yu, F. Yan, S. Liu, *et al.*, *Nature* **616**, 56 (2023).

[3] V. Sivak, A. Eickbusch, B. Royer, S. Singh, I. Tsoutsios, S. Ganjam, A. Miano, B. Brock, A. Ding, L. Frunzio, *et al.*, *Nature* **616**, 50 (2023).

[4] D. K. Tuckett, S. D. Bartlett, and S. T. Flammia, *Phys. Rev. Lett.* **120**, 050505 (2018).

[5] J. Zhang, Y.-C. Wu, and G.-P. Guo, *Physical Review A* **107** (2023), 10.1103/physreva.107.062408.

[6] K. Noh and C. Chamberland, *Phys. Rev. A* **101**, 012316 (2020).

[7] K. Noh, C. Chamberland, and F. G. Brandão, *PRX Quantum* **3**, 010315 (2022).

[8] K. Fukui, A. Tomita, A. Okamoto, and K. Fujii, *Phys. Rev. X* **8**, 021054 (2018).

[9] N. Raveendran, N. Rengaswamy, F. Rozpędek, A. Raina, L. Jiang, and B. Vasić, *Quantum* **6**, 767 (2022).

[10] L. Berent, T. Hillmann, J. Eisert, R. Wille, and J. Roffe, *PRX Quantum* **5**, 020349 (2024).

[11] D. Ruiz, J. Guillaud, A. Leverrier, M. Mirrahimi, and C. Vuillot, *Nature Communications* **16**, 1040 (2025).

[12] É. Gouzien, D. Ruiz, F.-M. Le Régent, J. Guillaud, and N. Sangouard, *Physical Review Letters* **131**, 040602 (2023).

[13] A. L. Grimsmo, J. Combes, and B. Q. Baragiola, *Physical Review X* **10** (2020), 10.1103/physrevx.10.011058.

[14] A. Denys and A. Leverrier, *Phys. Rev. Lett.* **133**, 240603 (2024).

[15] M. H. Michael, M. Silveri, R. Brierley, V. V. Albert, J. Salmilehto, L. Jiang, and S. M. Girvin, *Physical Review X* **6**, 031006 (2016).

[16] Even though the physical representation is given using the passive linear operations on the  $d$  modes, note its difference from the one given in [14], which assumes a physical representation that is isomorphic to the Pauli group itself while the one proposed here is more general.

[17] M. Bergmann and P. van Loock, *Phys. Rev. A* **94**, 012311 (2016).

[18] L. García-Álvarez, C. Calcluth, A. Ferraro, and G. Ferrini, *Phys. Rev. Res.* **2**, 043322 (2020).

[19] Y. Xu, Y. Wang, and V. V. Albert, *Phys. Rev. A* **110**, 022402 (2024).

[20] E. Descamps, A. Keller, and P. Milman, *Phys. Rev. Lett.* **132**, 170601 (2024).

[21] E. Knill, R. Laflamme, and G. J. Milburn, *Nature* **409**, 46 (2001).

[22] J. Guillaud and M. Mirrahimi, *Physical Review X* **9**, 041053 (2019).

[23] V. V. Albert, S. O. Mundhada, A. Grimm, S. Touzard, M. H. Devoret, and L. Jiang, *Quantum Science and Technology* **4**, 035007 (2019).

[24] S. S. Chelluri, S. Sharma, F. Schmidt, S. V. Kusminskiy, and P. van Loock, “*Bosonic quantum error correction with microwave cavities for quantum repeaters*,” (2025), arXiv:2503.21569 [quant-ph].

[25] Furthermore, our codes are also distinct from the bosonic quantum Fourier codes based on cat states along a similar group-theoretic construction [41].

[26] I. L. Chuang, D. W. Leung, and Y. Yamamoto, *Phys. Rev. A*

56, 1114 (1997).

[27] A. S. Fletcher, P. W. Shor, and M. Z. Win, *Physical Review A* **75** (2007), 10.1103/physreva.75.012338.

[28] A. Udupa, T. Hillmann, R. G. Ahmed, A. Smirne, and G. Ferrini, arXiv preprint arXiv:2505.08670 (2025).

[29] U. Leonhardt, J. A. Vaccaro, B. Böhmer, and H. Paul, *Phys. Rev. A* **51**, 84 (1995).

[30] J. Bergli, Y. M. Galperin, and B. L. Altshuler, *Phys. Rev. B* **74**, 024509 (2006).

[31] J. Bergli, Y. M. Galperin, and B. L. Altshuler, *New Journal of Physics* **11**, 025002 (2009).

[32] J. Schriefl, Y. Makhlin, A. Shnirman, and G. Schön, *New Journal of Physics* **8**, 1 (2006).

[33] C. Müller, J. H. Cole, and J. Lisenfeld, *Reports on Progress in Physics* **82**, 124501 (2019).

[34] C. Benedetti, M. G. Paris, and S. Maniscalco, *Physical Review A* **89**, 012114 (2014).

[35] R. Lescanne, M. Villiers, T. Peronnin, A. Sarlette, M. Delbecq, B. Huard, T. Kontos, M. Mirrahimi, and Z. Leghtas, *Nature Physics* **16**, 509 (2020).

[36] B. J. Chapman, S. J. de Graaf, S. H. Xue, Y. Zhang, J. Teoh, J. C. Curtis, T. Tsunoda, A. Eickbusch, A. P. Read, A. Koottandavida, S. O. Mundhada, L. Frunzio, M. Devoret, S. Girvin, and R. Schoelkopf, *PRX Quantum* **4**, 020355 (2023).

[37] B. Royer, S. Singh, and S. Girvin, *PRX Quantum* **3**, 010335 (2022).

[38] Nordquantique, “*Suppressing logical errors with multimode quantum error correction*,” (2025).

[39] T. Hillmann, F. Quijandría, G. Johansson, A. Ferraro, S. Gasparinetti, and G. Ferrini, *Physical review letters* **125**, 160501 (2020).

[40] A. M. Eriksson, T. Sépulcre, M. Kervinen, T. Hillmann, M. Kudra, S. Dupouy, Y. Lu, M. Khanahmadi, J. Yang, C. Castillo-Moreno, *et al.*, *Nature Communications* **15**, 2512 (2024).

[41] A. Leverrier, “*Bosonic quantum fourier codes*,” (2025), arXiv:2505.16618 [quant-ph].

[42] T. Hillmann, F. Quijandría, A. L. Grimsmo, and G. Ferrini, *PRX Quantum* **3**, 020334 (2022).

## Appendix A: Multimode rotation-symmetric codewords

In this section, we provide a derivation of the qudit codewords Eq. (3). Firstly, note that unlike [14] where both the group  $G$  and the physical representation  $\pi$  are isomorphic to the Pauli group, we have utilised the fact that it is sufficient for there to exist a homomorphism,  $\lambda$ , from  $G$  to the Pauli group and a physical representation,  $\pi$ , that acts as  $\lambda$  on at least one two-dimensional subspace.

For the derivation it suffices to work out the case for  $\hat{U}_{BS} = \mathbb{I}$ . We start by considering the general superposition of all possible states supported by  $d$  modes, given by

$$|k_N\rangle = \sum_{\{m_i\}=0}^{\infty} f_{m_0, \dots, m_{d-1}}^{(k)} |m_0, m_1, \dots, m_{d-1}\rangle. \quad (\text{A1})$$

By imposing that the physical representation of the group element  $h$  acts as in Eq.(2), i.e. that  $\pi(h)|k_N\rangle = e^{i\frac{2\pi}{N}d} |k_N\rangle = \omega_d^k |k_N\rangle$ , with  $\omega_d = e^{2\pi i/d}$ , we find,

$$\begin{aligned} f_{m_0, \dots, m_{d-1}}^{(k)} &= 0, \text{ unless } e^{i\frac{2\pi}{N}d m_0} = e^{i\frac{2\pi k}{d}} \\ &\implies m_0 = (n_0 d + k)N, \forall n_0 \in \mathbb{N}_0. \end{aligned} \quad (\text{A2})$$

By imposing the physical representation of group element  $g$ , we require that  $\pi(g)|k_N\rangle = |(k \oplus 1)_N\rangle$ . Using the relation,  $e^{i\frac{\pi}{2}\hat{G}_{i,i+1}^-} e^{-i\frac{\pi}{2}\hat{G}_{i,i+1}^-} = -\hat{a}_{i+1}^\dagger$ , we obtain

$$f_{m_0, \dots, m_{d-1}}^{(k)} (-1)^{\sum_{i=1}^{d-1} m_i} = f_{m_1, \dots, m_{d-1}, m_0}^{(k \oplus 1)}. \quad (\text{A3})$$

From Eq. (A2), we also see that  $f_{m_1, \dots, m_{d-1}, m_0}^{(k \oplus 1)} = 0$ , unless  $m_1 = [n_1 d + (k \oplus 1)]N$ . This implies

$$f_{m_0, \dots, m_{d-1}}^{(k)} = 0, \text{ unless } m_1 = [n_1 d + (k \oplus 1)]N. \quad (\text{A4})$$

Similarly applying  $\pi(g)$  on  $|k \oplus 1\rangle$ , we arrive at the condition  $f_{m_1, \dots, m_0}^{(k \oplus 1)} (-1)^{\sum_{i=1}^{d-1} m_i} = f_{m_2, \dots, m_0, m_1}^{(k \oplus 2)}$  where we again use Eq. (A2) to obtain the fact that  $f_{m_2, \dots, m_1}^{(k \oplus 2)}$ , and thus  $f_{m_0, \dots, m_{d-1}}^{(k)}$  is equal to 0, unless  $m_2 = [n_2 d + (k \oplus 2)]N$ .

By induction, we therefore have

$$f_{m_0, \dots, m_j, \dots, m_{d-1}}^{(k)} = 0, \text{ unless } m_j = [n_j d + (k \oplus j)]N \quad (\text{A5})$$

for all  $j = 0, \dots, d-1$ . Furthermore, since  $N$  is an even number,  $(-1)^{\sum_{i=1}^{d-1} m_i} = 1$  for all the fock-states that have non-zero amplitudes in the codewords. The codewords thus take the form given in Eq. (3).

### Appendix B: The effective noise channel up to first order in noise strengths

The set-up and the error correction procedure that we investigate in this paper is given as follows (see Figure 4). First, we prepare the logical state  $\hat{\rho}$  in the two-mode encoding in the modes through which noise occurs ( $\hat{a}_1, \hat{a}_2$ ). Hence,

$$\hat{\rho} = \sum_{i,j=0}^1 \rho_{ij} |i_N\rangle\langle j_N|. \quad (\text{B1})$$

Then we apply a beam-splitter action,  $\hat{U}_{BS} = \exp \left[ i\delta(\hat{G}_{12}^+ \sin \phi + \hat{G}_{12}^- \cos \phi) \right] = \exp \left[ \delta(\hat{a}_2^\dagger \hat{a}_1 e^{i\phi} - \hat{a}_1^\dagger \hat{a}_2 e^{-i\phi}) \right]$ , let the system go through the noise channel  $\mathcal{N} = \mathcal{N}_L \circ \mathcal{N}_D$ , and then apply the inverse beam-splitter action  $\hat{U}_{BS}^\dagger$  before continuing with rest of the recovery operation,  $\tilde{\mathcal{R}}$ , where we have  $\mathcal{R}(\hat{\rho}) = \tilde{\mathcal{R}}(\hat{U}_{BS}^\dagger \hat{\rho} \hat{U}_{BS})$ . The beam-splitter transforms the two modes  $\hat{a}_1$  and  $\hat{a}_2$  into

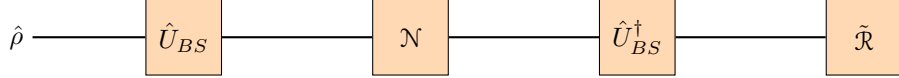


FIG. 4: An encoding and error-correcting procedure for the rotation-symmetric codes on two modes.

$\hat{b}_1$  and  $\hat{b}_2$  as follows

$$\hat{b}_1 = \hat{U}_{BS}^\dagger \hat{a}_1 \hat{U}_{BS} = \hat{a}_1 \cos \delta + \hat{a}_2 e^{-i\phi} \sin \delta \quad (\text{B2})$$

$$\hat{b}_2 = \hat{U}_{BS}^\dagger \hat{a}_2 \hat{U}_{BS} = \hat{a}_2 \cos \delta - \hat{a}_1 e^{i\phi} \sin \delta. \quad (\text{B3})$$

With the Kraus representation provided in Eq.(8), the evolution of a state under these channels can be written as

$$\begin{aligned} \tilde{\mathcal{N}}(\hat{\rho}) &= \hat{U}_{BS}^\dagger \mathcal{N}(\hat{U}_{BS} \hat{\rho} \hat{U}_{BS}^\dagger) \hat{U}_{BS} \\ &= \sum_{p,q,r,s=0}^{\infty} \hat{U}_{BS}^\dagger \hat{L}_p^{(1)} \hat{L}_q^{(2)} \hat{D}_r^{(1)} \hat{D}_s^{(2)} \hat{U}_{BS} \hat{\rho} \hat{U}_{BS}^\dagger \hat{D}_s^{(2)\dagger} \hat{D}_r^{(1)\dagger} \hat{L}_q^{(2)\dagger} \hat{L}_p^{(1)\dagger} \hat{U}_{BS}. \end{aligned} \quad (\text{B4})$$

Note that the modified noise channel under the beam-splitter operation is denoted by  $\tilde{\mathcal{N}}$  instead of  $\mathcal{N}$ . We can further re-write

$$\hat{U}_{BS}^\dagger \hat{L}_p^{(1)} \hat{L}_q^{(2)} \hat{D}_r^{(1)} \hat{D}_s^{(2)} \hat{U}_{BS} = \hat{\tilde{L}}_p^{(1)} \hat{\tilde{L}}_q^{(2)} \hat{\tilde{D}}_r^{(1)} \hat{\tilde{D}}_s^{(2)}, \quad (\text{B5})$$

where, using Eq.(10), the new Kraus operators are

$$\hat{\tilde{L}}_p^{(1)} = \sqrt{\frac{(1 - e^{-\kappa_1 t})^p}{p!}} e^{-\frac{1}{2}\kappa_1 t} \hat{b}_1^\dagger \hat{b}_1 \hat{b}_1^p \quad \hat{\tilde{L}}_q^{(2)} = \sqrt{\frac{(1 - e^{-\kappa_2 t})^q}{q!}} e^{-\frac{1}{2}\kappa_2 t} \hat{b}_2^\dagger \hat{b}_2 \hat{b}_2^q \quad (\text{B6})$$

$$\hat{\tilde{D}}_r^{(1)} = \sqrt{\frac{(\gamma_1 t)^r}{r!}} e^{-\frac{1}{2}\gamma_1 t} (\hat{b}_1^\dagger \hat{b}_1)^2 (\hat{b}_1^\dagger \hat{b}_1)^r \quad \hat{\tilde{D}}_s^{(2)} = \sqrt{\frac{(\gamma_2 t)^s}{s!}} e^{-\frac{1}{2}\gamma_2 t} (\hat{b}_2^\dagger \hat{b}_2)^2 (\hat{b}_2^\dagger \hat{b}_2)^s. \quad (\text{B7})$$

The recovery procedure involves a non-destructive modular number measurement to detect the error syndrome and a corresponding unitary operator is applied. This modular number measurement in each of the modes is defined by the following set of POVMs:  $\{\hat{P}_l \otimes \hat{P}_m : l, m = 0, 1\}$  where  $\hat{P}_i := \sum_{n=0}^{\infty} |Nn+i\rangle\langle Nn+i|$  [13, 15]. We intend to find the recovery map that corrects the error induced by the noise channel up to the first order in the noise strengths,  $\kappa_i t$  and  $\gamma_i t$  corresponding to the loss and dephasing channel respectively. We expand the effect of the resulting map,  $\tilde{\mathcal{N}}$ , up to the first order in the noise strengths,  $\kappa_i t$  and  $\gamma_i t$ , and identify the terms that are non-vanishing under the modular number measurement [13, 15]. Up to the first order in

$\kappa_i t$  and  $\gamma_i t$ , the effect of the noise channel can be written as

$$\begin{aligned}\tilde{N}(\hat{\rho}) \approx \hat{\rho} - \frac{\kappa_1 t}{2} \{ \hat{b}_1^\dagger \hat{b}_1, \hat{\rho} \} - \frac{\kappa_2 t}{2} \{ \hat{b}_2^\dagger \hat{b}_2, \hat{\rho} \} - \frac{\gamma_1 t}{2} \{ (\hat{b}_1^\dagger \hat{b}_1)^2, \hat{\rho} \} - \frac{\gamma_2 t}{2} \{ (\hat{b}_2^\dagger \hat{b}_2)^2, \hat{\rho} \} \\ + \kappa_1 t \hat{b}_1 \hat{\rho} \hat{b}_1^\dagger + \kappa_2 t \hat{b}_2 \hat{\rho} \hat{b}_2^\dagger + \gamma_1 t (\hat{b}_1^\dagger \hat{b}_1) \hat{\rho} (\hat{b}_1^\dagger \hat{b}_1) + \gamma_2 t (\hat{b}_2^\dagger \hat{b}_2) \hat{\rho} (\hat{b}_2^\dagger \hat{b}_2).\end{aligned}\quad (\text{B8})$$

Further,

$$\hat{b}_1^\dagger \hat{b}_1 = \hat{a}_1^\dagger \hat{a}_1 \cos^2 \delta + \hat{a}_2^\dagger \hat{a}_2 \sin^2 \delta + (e^{-i\phi} \hat{a}_1^\dagger \hat{a}_2 + e^{i\phi} \hat{a}_2^\dagger \hat{a}_1) \sin \delta \cos \delta \quad (\text{B9})$$

$$\hat{b}_2^\dagger \hat{b}_2 = \hat{a}_2^\dagger \hat{a}_2 \cos^2 \delta + \hat{a}_1^\dagger \hat{a}_1 \sin^2 \delta - (e^{-i\phi} \hat{a}_1^\dagger \hat{a}_2 + e^{i\phi} \hat{a}_2^\dagger \hat{a}_1) \sin \delta \cos \delta. \quad (\text{B10})$$

Therefore, we have for the terms coming from the loss channel

$$\begin{aligned}\frac{\kappa_1 t}{2} \{ \hat{b}_1^\dagger \hat{b}_1, \hat{\rho} \} + \frac{\kappa_2 t}{2} \{ \hat{b}_2^\dagger \hat{b}_2, \hat{\rho} \} &= \frac{1}{2} \{ (\kappa_1 \hat{b}_1^\dagger \hat{b}_1 + \kappa_2 \hat{b}_2^\dagger \hat{b}_2) t, \hat{\rho} \} \\ &= \frac{1}{2} \underbrace{\{ [(\kappa_1 t \cos^2 \delta + \kappa_2 t \sin^2 \delta) \hat{a}_1^\dagger \hat{a}_1 + (\kappa_2 t \cos^2 \delta + \kappa_1 t \sin^2 \delta) \hat{a}_2^\dagger \hat{a}_2], \hat{\rho} \}}_{\text{No jump}} \\ &\quad + \frac{1}{2} \underbrace{\{ [(\kappa_1 t - \kappa_2 t) (e^{-i\phi} \hat{a}_1^\dagger \hat{a}_2 + e^{i\phi} \hat{a}_2^\dagger \hat{a}_1) \sin \delta \cos \delta], \hat{\rho} \}}_{\text{Vanishes under modular number measurements}}\end{aligned}\quad (\text{B11})$$

and

$$\begin{aligned}\kappa_1 t \hat{b}_1 \hat{\rho} \hat{b}_1^\dagger + \kappa_2 t \hat{b}_2 \hat{\rho} \hat{b}_2^\dagger \\ = \underbrace{(\kappa_1 t \cos^2 \delta + \kappa_2 t \sin^2 \delta) \hat{a}_1 \hat{\rho} \hat{a}_1^\dagger + (\kappa_2 t \cos^2 \delta + \kappa_1 t \sin^2 \delta) \hat{a}_2 \hat{\rho} \hat{a}_2^\dagger}_{\text{Single photon loss in either mode}} \\ + \text{A part that vanishes under modular number measurements}\end{aligned}\quad (\text{B12})$$

Note that in this first-order expansion all non-vanishing terms are independent on  $\phi$ .

Similarly, from the dephasing channel

$$\begin{aligned}\frac{\gamma_1 t}{2} \{ (\hat{b}_1^\dagger \hat{b}_1)^2, \hat{\rho} \} + \frac{\gamma_2 t}{2} \{ (\hat{b}_2^\dagger \hat{b}_2)^2, \hat{\rho} \} \\ = \frac{1}{2} \underbrace{\{ [\gamma_1 t (\hat{a}_1^\dagger \hat{a}_1 \cos^2 \delta + \hat{a}_2^\dagger \hat{a}_2 \sin^2 \delta)^2 + \gamma_2 t (\hat{a}_2^\dagger \hat{a}_2 \cos^2 \delta + \hat{a}_1^\dagger \hat{a}_1 \sin^2 \delta)^2], \hat{\rho} \}}_{\text{No jump}} \\ + \frac{1}{2} \underbrace{\{ (\gamma_1 t + \gamma_2 t) (\hat{a}_1^\dagger \hat{a}_2 \hat{a}_2^\dagger \hat{a}_1 + \hat{a}_2^\dagger \hat{a}_1 \hat{a}_1^\dagger \hat{a}_2) \sin^2 \delta \cos^2 \delta, \hat{\rho} \}}_{\text{No jump}} \\ + \frac{1}{2} \underbrace{\{ (\gamma_1 t + \gamma_2 t) [(\hat{a}_1^\dagger \hat{a}_2)^2 e^{-2i\phi} + (\hat{a}_2^\dagger \hat{a}_1)^2 e^{2i\phi}] \sin^2 \delta \cos^2 \delta, \hat{\rho} \}}_{\text{No jump for only } N = 2; \text{ otherwise vanishes under modular number measurements}} \\ + \text{A part that vanishes under modular number measurements}\end{aligned}\quad (\text{B13})$$

and

$$\begin{aligned}\gamma_1 t (\hat{b}_1^\dagger \hat{b}_1) \hat{\rho} (\hat{b}_1^\dagger \hat{b}_1) + \gamma_2 t (\hat{b}_2^\dagger \hat{b}_2) \hat{\rho} (\hat{b}_2^\dagger \hat{b}_2) \\ = \underbrace{\gamma_1 t (\hat{a}_1^\dagger \hat{a}_1 \cos^2 \delta + \hat{a}_2^\dagger \hat{a}_2 \sin^2 \delta) \hat{\rho} (\hat{a}_1^\dagger \hat{a}_1 \cos^2 \delta + \hat{a}_2^\dagger \hat{a}_2 \sin^2 \delta)}_{\text{No jump}} \\ + \underbrace{\gamma_2 t (\hat{a}_2^\dagger \hat{a}_2 \cos^2 \delta + \hat{a}_1^\dagger \hat{a}_1 \sin^2 \delta) \hat{\rho} (\hat{a}_2^\dagger \hat{a}_2 \cos^2 \delta + \hat{a}_1^\dagger \hat{a}_1 \sin^2 \delta)}_{\text{No jump}} \\ + \underbrace{(\gamma_1 t + \gamma_2 t) [\hat{a}_1^\dagger \hat{a}_2 \hat{\rho} \hat{a}_2^\dagger \hat{a}_1 + \hat{a}_2^\dagger \hat{a}_1 \hat{\rho} \hat{a}_1^\dagger \hat{a}_2] \sin^2 \delta \cos^2 \delta}_{\text{Single photon exchange}} \\ + \text{A part that vanishes under modular number measurements}\end{aligned}\quad (\text{B14})$$

Note that even in this case, the dependency on  $\phi$  only occurs in the case of  $N = 2$ , while for any other even  $N$  the first-order

expansion is independent of  $\phi$ .

Based on this expansion, we give recovery procedures in the presence of purely loss and purely dephasing channels in Appendices C and D respectively, for the specific values of  $N$  and  $K$  of the encoding mentioned.

### Appendix C: Recovery of $K = 2, N = 2$ code and $K = 2, N = 4$ against loss channel

Here we derived the state recovery maps for the smallest instances of two-mode binomial codes. Note that in view of Eq.(B4) we are going to consider the non-rotated codewords, while the mixing operations  $\hat{U}_{BS}(\delta, \phi)$  has been absorbed in the error channel.

#### 1. $K = 2, N = 2$ binomial encoding

The smallest encoding, the  $K = 2, N = 2$  code, has the following codewords:

$$|0_N\rangle = \frac{1}{\sqrt{2}}(|0\rangle + |4\rangle) \otimes |2\rangle, \quad (\text{C1})$$

$$|1_N\rangle = |2\rangle \otimes \frac{1}{\sqrt{2}}(|0\rangle + |4\rangle). \quad (\text{C2})$$

The projector onto the codespace is defined as

$$\hat{P}_C = |0_N\rangle\langle 0_N| + |1_N\rangle\langle 1_N|.$$

The modular number measurement in each mode is described by the POVM set

$$\{\hat{P}_l \otimes \hat{P}_m : l, m = 0, 1\}, \quad \hat{P}_i := \sum_{n=0}^{\infty} |2n+i\rangle\langle 2n+i|. \quad (\text{C3})$$

From Eqs. (B11) and (B12), we write  $\tilde{\mathcal{N}}(\hat{\rho}) = \hat{\rho} - \hat{M}(\hat{\rho})$  where the the leading-order contribution of the loss channel that survives under modular measurements is

$$\hat{M}(\hat{\rho}) = \{\hat{M}_0, \hat{\rho}\} - \hat{M}_1 \hat{\rho} \hat{M}_1^\dagger - \hat{M}_2 \hat{\rho} \hat{M}_2^\dagger, \quad (\text{C4})$$

where

$$\hat{M}_0 = \frac{1}{2} \left( (\kappa_1 t \cos^2 \delta + \kappa_2 t \sin^2 \delta) \hat{a}_1^\dagger \hat{a}_1 + (\kappa_2 t \cos^2 \delta + \kappa_1 t \sin^2 \delta) \hat{a}_2^\dagger \hat{a}_2 \right), \quad (\text{C5})$$

$$\hat{M}_1 = \sqrt{(\kappa_1 t \cos^2 \delta + \kappa_2 t \sin^2 \delta)} \hat{a}_1, \quad (\text{C6})$$

$$\hat{M}_2 = \sqrt{(\kappa_2 t \cos^2 \delta + \kappa_1 t \sin^2 \delta)} \hat{a}_2. \quad (\text{C7})$$

Here, terms with  $\hat{M}_0$  correspond to the error syndrome  $l = 0, m = 0$  (*no-jump events*), while  $\hat{M}_1$  and  $\hat{M}_2$  correspond to *single-photon loss* in the first and second modes, detected when  $l = 1, m = 0$  and  $l = 0, m = 1$ , respectively. Noise operators associated with  $l = 1, m = 1$  arise only at higher order, scaling as  $(\kappa_i t)^2$ .

**Knill–Laflamme conditions:** We first verify that the first-order error operators satisfy the Knill–Laflamme (KL) conditions. For two noise operators  $\hat{E}_1$  and  $\hat{E}_2$ , we check if  $\hat{P}_C \hat{E}_2^\dagger \hat{E}_1 \hat{P}_C$  is proportional to  $\hat{P}_C$ . Here we show the evaluation of the possible combinations for  $E_1$  and  $E_2$  for the non-trivial cases only. The other cases can be similarly checked. For the first term in Eq. (C4), choosing  $\hat{E}_1 = \hat{M}_0$  and  $\hat{E}_2 = \mathbb{I}^{\otimes 2}$  (which appears in the first order), and setting

$$A = \frac{1}{2}(\kappa_1 t \cos^2 \delta + \kappa_2 t \sin^2 \delta), \quad B = \frac{1}{2}(\kappa_2 t \cos^2 \delta + \kappa_1 t \sin^2 \delta),$$

such that  $\hat{M}_0 = A\hat{a}_1^\dagger\hat{a}_1 + B\hat{a}_2^\dagger\hat{a}_2$ . By looking at the action of the operators  $\hat{a}_1^\dagger\hat{a}_1$  and  $\hat{a}_2^\dagger\hat{a}_2$  on the codewords, we obtain

$$\hat{a}_1^\dagger\hat{a}_1|0_N\rangle = \frac{1}{\sqrt{2}}4|4\rangle \otimes |2\rangle, \quad (\text{C8})$$

$$\hat{a}_1^\dagger\hat{a}_1|1_N\rangle = 2|2\rangle \otimes \frac{1}{\sqrt{2}}(|0\rangle + |4\rangle), \quad (\text{C9})$$

$$\hat{a}_2^\dagger\hat{a}_2|0_N\rangle = \frac{1}{\sqrt{2}}(|0\rangle + |4\rangle) \otimes 2|2\rangle, \quad (\text{C10})$$

$$\hat{a}_2^\dagger\hat{a}_2|1_N\rangle = |2\rangle \otimes \frac{1}{\sqrt{2}}4|4\rangle, \quad (\text{C11})$$

from which we obtain

$$\langle 0_N| \hat{a}_1^\dagger\hat{a}_1|0_N\rangle = \langle 1_N| \hat{a}_1^\dagger\hat{a}_1|1_N\rangle = \langle 0_N| \hat{a}_2^\dagger\hat{a}_2|0_N\rangle = \langle 1_N| \hat{a}_2^\dagger\hat{a}_2|1_N\rangle = 2, \quad (\text{C12})$$

while the off-diagonal elements are zero. Therefore, from Eqs. (C8)–(C12), the matrix elements  $\langle i_N| \hat{M}_0| i_N\rangle$  vanish for  $i \neq j$ , while for  $i = j$ , we have  $\langle i_N| \hat{M}_0| i_N\rangle = 2A + 2B$ . The action of the projector  $\hat{P}_C$  on the operator  $\hat{M}_0$  gives therefore

$$\hat{P}_C\hat{M}_0\hat{P}_C = \sum_{i,j=0,1} \langle i_N| \hat{M}_0| j_N\rangle |i_N\rangle \langle j_N| = \sum_{i=0,1} (2A + 2B)|i_N\rangle \langle i_N| = (2A + 2B)\hat{P}_C. \quad (\text{C13})$$

Thus, the KL conditions are satisfied.

Next, for *single-photon loss*, choosing  $\hat{E}_1 = \hat{M}_1$  and  $\hat{E}_2 = \hat{M}_2$ , their action on the codewords is

$$\hat{a}_1|0_N\rangle = \frac{1}{\sqrt{2}}\sqrt{4}|3\rangle \otimes |2\rangle, \quad (\text{C14})$$

$$\hat{a}_1|1_N\rangle = \sqrt{2}|1\rangle \otimes \frac{1}{\sqrt{2}}(|0\rangle + |4\rangle), \quad (\text{C15})$$

$$\hat{a}_2|0_N\rangle = \frac{1}{\sqrt{2}}(|0\rangle + |4\rangle) \otimes \sqrt{2}|1\rangle, \quad (\text{C16})$$

$$\hat{a}_2|1_N\rangle = |2\rangle \otimes \frac{1}{\sqrt{2}}\sqrt{4}|3\rangle. \quad (\text{C17})$$

From Eqs. (C14)–(C17), one verifies that  $\langle i_N| \hat{M}_1^\dagger\hat{M}_2| j_N\rangle = 0$  for all  $i, j$ , and hence the KL conditions are again satisfied:

$$\hat{P}_C\hat{M}_1^\dagger\hat{M}_2\hat{P}_C \propto \hat{P}_C. \quad (\text{C18})$$

**Recovery map:** We now provide the unitary recovery maps corresponding to these error syndromes. The unitaries correcting the errors  $\hat{M}_0$ ,  $\hat{M}_1$ , and  $\hat{M}_2$  are denoted by  $\hat{U}_{00}$ ,  $\hat{U}_{10}$ , and  $\hat{U}_{01}$ , respectively. They are defined as

$$\hat{U}_{00} = \exp([\hat{M}_0, \hat{P}_C]), \quad (\text{C19})$$

whose first-order expansion in  $\kappa_i t$  is

$$\hat{U}_{00} = \mathbb{I}^{\otimes 2} + [\hat{M}_0, \hat{P}_C]. \quad (\text{C20})$$

For single-photon loss, we have

$$\hat{U}_{10} = \left( \frac{1}{\sqrt{2}}(|0\rangle + |4\rangle)\langle 3| + |2\rangle\langle 1| + \hat{U}_{1,\text{res}} \right) \otimes \mathbb{I}, \quad (\text{C21})$$

$$\hat{U}_{01} = \mathbb{I} \otimes \left( \frac{1}{\sqrt{2}}(|0\rangle + |4\rangle)\langle 3| + |2\rangle\langle 1| + \hat{U}_{1,\text{res}} \right), \quad (\text{C22})$$

where  $\hat{U}_{1,\text{res}}$  is a complementary operator ensuring unitarity. As mentioned before, measurement outcomes with  $l = 1, m = 1$  appear only at order  $(\kappa_i t)^2$ ; hence no correction is applied:

$$\hat{U}_{11} = \mathbb{I} \otimes \mathbb{I}. \quad (\text{C23})$$

The complete recovery map has the Kraus representation

$$\tilde{\mathcal{R}} \sim \left\{ \hat{U}_{lm} (\hat{P}_l \otimes \hat{P}_m) \right\}. \quad (\text{C24})$$

**Verification of recovery map:** We now verify that Eq. (C24) recovers the initial state  $\hat{\rho}$ . For *no-jump*, expanding consistently to first order in  $\kappa_i t$  gives

$$\begin{aligned} & \hat{U}_{00} (\hat{P}_0 \otimes \hat{P}_0) \tilde{\mathcal{N}}(\hat{\rho}) (\hat{P}_0 \otimes \hat{P}_0) \hat{U}_{00}^\dagger \\ &= (\mathbb{I}^{\otimes 2} + [\hat{M}_0, \hat{P}_C]) (\hat{\rho} - \{\hat{M}_0, \hat{\rho}\}) (\mathbb{I}^{\otimes 2} - [\hat{M}_0, \hat{P}_C]) \\ &= \hat{\rho} - \{\hat{M}_0, \hat{\rho}\} + [\hat{M}_0, \hat{P}_C] \hat{\rho} - \hat{\rho} [\hat{M}_0, \hat{P}_C] \\ &= \hat{\rho} - \{\hat{P}_C \hat{M}_0 \hat{P}_C, \hat{\rho}\} \\ &= \hat{\rho} - \left\{ (\kappa_1 t \cos^2 \delta + \kappa_2 t \sin^2 \delta) + (\kappa_2 t \cos^2 \delta + \kappa_1 t \sin^2 \delta), \hat{\rho} \right\} \\ &= \hat{\rho} - 2(\kappa_1 t + \kappa_2 t) \hat{\rho}, \end{aligned} \quad (\text{C25})$$

where we have used  $P_c \hat{\rho} = \hat{\rho}$ , and that the Hermitian conjugate of a commutator takes a minus sign. For *single-photon loss*, again neglecting  $\mathcal{O}((\kappa_i t)^2)$  contributions, we obtain

$$\hat{U}_{10} (\hat{P}_1 \otimes \hat{P}_0) \tilde{\mathcal{N}}(\hat{\rho}) (\hat{P}_1 \otimes \hat{P}_0) \hat{U}_{10}^\dagger + \hat{U}_{01} (\hat{P}_0 \otimes \hat{P}_1) \tilde{\mathcal{N}}(\hat{\rho}) (\hat{P}_0 \otimes \hat{P}_1) \hat{U}_{01}^\dagger = 2(\kappa_1 t + \kappa_2 t) \hat{\rho}. \quad (\text{C26})$$

Thus, the recovered state is

$$\tilde{\mathcal{R}} \circ \tilde{\mathcal{N}}(\hat{\rho}) = \hat{\rho} + \mathcal{O}((\kappa_i t)^2). \quad (\text{C27})$$

## 2. $K = 2, N = 4$ binomial encoding

The two-mode  $K = 2, N = 4$  binomial code is defined by the logical states

$$|0_N\rangle = \frac{1}{\sqrt{2}}(|0\rangle + |8\rangle) \otimes |4\rangle, \quad (\text{C28})$$

$$|1_N\rangle = |4\rangle \otimes \frac{1}{\sqrt{2}}(|0\rangle + |8\rangle). \quad (\text{C29})$$

The modular number measurement for the two modes corresponds to the projective set

$$\{\hat{P}_l \otimes \hat{P}_m : l, m = 0, 1, 2, 3\}, \quad \hat{P}_l = \sum_{n=0}^{\infty} |4n+l\rangle\langle 4n+l|. \quad (\text{C30})$$

**Knill–Laflamme conditions:** It can be verified that the Knill–Laflamme conditions for the loss channel, up to first order, are satisfied in this case as well, following steps analogous to the  $K = 2, N = 2$  code. We therefore omit the detailed calculation.

**Recovery map:** The no-jump part of  $\hat{M}(\hat{\rho})$ , denoted  $\hat{M}_0(\hat{\rho})$ , can be corrected by the unitary

$$\hat{U}_{00} = \exp([\hat{M}_0, \hat{P}_C]), \quad (\text{C31})$$

which expands to first order as

$$\hat{U}_{00} = \mathbb{I}^{\otimes 2} + [\hat{M}_0, \hat{P}_C] + \mathcal{O}((\kappa_i t)^2). \quad (\text{C32})$$

The error components  $\hat{M}_1(\hat{\rho})$  and  $\hat{M}_2(\hat{\rho})$  can be corrected with the unitaries

$$\hat{U}_{10} = \left( \frac{1}{\sqrt{2}}(|0\rangle + |8\rangle)\langle 7| + |4\rangle\langle 3| + \hat{U}_{1,\text{res}} \right) \otimes \mathbb{I}, \quad (\text{C33})$$

$$\hat{U}_{01} = \mathbb{I} \otimes \left( \frac{1}{\sqrt{2}}(|0\rangle + |8\rangle)\langle 7| + |4\rangle\langle 3| + \hat{U}_{1,\text{res}} \right), \quad (\text{C34})$$

where  $\hat{U}_{1,\text{res}}$  is a complementary operator that ensures unitarity of  $\hat{U}_1$ . The complete recovery map again admits a Kraus

representation,

$$\tilde{\mathcal{R}} \sim \left\{ \hat{U}_{lm} (\hat{P}_l \otimes \hat{P}_m) \right\}. \quad (\text{C35})$$

**Verification of the recovery map:** We now check that the recovery map corrects the noisy state up to first order. The action of the unitaries after modular measurements yields

$$\hat{U}_{00}(\hat{P}_0 \otimes \hat{P}_0)\tilde{\mathcal{N}}(\hat{\rho})(\hat{P}_0 \otimes \hat{P}_0)\hat{U}_{00}^\dagger = \hat{\rho} - 4(\kappa_1 t + \kappa_2 t)\hat{\rho} + \mathcal{O}((\kappa_i t)^2), \quad (\text{C36})$$

$$\hat{U}_{10}(\hat{P}_1 \otimes \hat{P}_0)\tilde{\mathcal{N}}(\hat{\rho})(\hat{P}_1 \otimes \hat{P}_0)\hat{U}_{10}^\dagger + \hat{U}_{01}(\hat{P}_0 \otimes \hat{P}_1)\tilde{\mathcal{N}}(\hat{\rho})(\hat{P}_0 \otimes \hat{P}_1)\hat{U}_{01}^\dagger = 4(\kappa_1 t + \kappa_2 t)\hat{\rho} + \mathcal{O}((\kappa_i t)^2). \quad (\text{C37})$$

Thus, the total recovered state is

$$\tilde{\mathcal{R}} \circ \tilde{\mathcal{N}}(\hat{\rho}) = \hat{\rho} + \mathcal{O}((\kappa_i t)^2). \quad (\text{C38})$$

## Appendix D: Recovery of $K = 2, N = 2$ code and $K = 2, N = 4$ against dephasing channel

### 1. $K = 2, N = 2$ binomial encoding

We refer again to the set of POVM elements in Eq.(C3) for the syndrome measurement. From Eqs. (B13) and (B14), the evolution of a state encoded with  $K = 2, N = 2$  under the dephasing channel is given by  $\tilde{\mathcal{N}}(\hat{\rho}) = \hat{\rho} - \hat{M}(\hat{\rho})$  and up to first order in noise strength  $\gamma_i t$ , we have

$$\hat{M}(\hat{\rho}) = \{\hat{M}_0, \hat{\rho}\} - \hat{M}_0^{(1)}\hat{\rho}\hat{M}_0^{(1)\dagger} - \hat{M}_0^{(2)}\hat{\rho}\hat{M}_0^{(2)\dagger} - \hat{M}_1\hat{\rho}\hat{M}_1^\dagger - \hat{M}_2\hat{\rho}\hat{M}_2^\dagger, \quad (\text{D1})$$

where

$$\begin{aligned} \hat{M}_0 &= \frac{1}{2} \left( \gamma_1 t (\hat{a}_1^\dagger \hat{a}_1 \cos^2 \delta + \hat{a}_2^\dagger \hat{a}_2 \sin^2 \delta)^2 + \gamma_2 t (\hat{a}_2^\dagger \hat{a}_2 \cos^2 \delta + \hat{a}_1^\dagger \hat{a}_1 \sin^2 \delta)^2 \right) \\ &\quad + \frac{1}{2} (\gamma_1 t + \gamma_2 t) (\hat{a}_1^\dagger \hat{a}_2 \hat{a}_2^\dagger \hat{a}_1 + \hat{a}_2^\dagger \hat{a}_1 \hat{a}_1^\dagger \hat{a}_2) \sin^2 \delta \cos^2 \delta \\ &\quad + \frac{1}{2} (\gamma_1 t + \gamma_2 t) ((\hat{a}_1^\dagger \hat{a}_2)^2 e^{-2i\phi} + (\hat{a}_2^\dagger \hat{a}_1)^2 e^{2i\phi}) \sin^2 \delta \cos^2 \delta, \end{aligned} \quad (\text{D2})$$

$$\hat{M}_0^{(1)} = \gamma_1 t (\hat{a}_1^\dagger \hat{a}_1 \cos^2 \delta + \hat{a}_2^\dagger \hat{a}_2 \sin^2 \delta), \quad (\text{D3})$$

$$\hat{M}_0^{(2)} = \gamma_2 t (\hat{a}_2^\dagger \hat{a}_2 \cos^2 \delta + \hat{a}_1^\dagger \hat{a}_1 \sin^2 \delta), \quad (\text{D4})$$

$$\hat{M}_1 = (\gamma_1 t + \gamma_2 t) (\hat{a}_1^\dagger \hat{a}_2) \sin \delta \cos \delta, \quad (\text{D5})$$

$$\hat{M}_2 = (\gamma_1 t + \gamma_2 t) (\hat{a}_2^\dagger \hat{a}_1) \sin \delta \cos \delta. \quad (\text{D6})$$

Here, the terms  $\hat{M}_0$ ,  $\hat{M}_0^{(1)}$ , and  $\hat{M}_0^{(2)}$  correspond to *no-jump* events associated with modular measurement outcomes  $l = 0, m = 0$ , while  $\hat{M}_1$  and  $\hat{M}_2$  correspond to *single-photon exchange* with syndromes  $l = 1, m = 1$ .

**Knill–Laflamme conditions:** We check the Knill–Laflamme conditions for the non-trivial cases. For the anticommutator term  $\{\hat{M}_0, \hat{\rho}\}$ , choosing  $\hat{E}_1 = \hat{M}_0$  and  $\hat{E}_2 = \mathbb{I}^{\otimes 2}$ , the first term in Eq. (D2) satisfies the KL condition when  $\delta = \pi/4, 3\pi/4$ :

$$\hat{P}_C \frac{(\gamma_1 t + \gamma_2 t)}{8} (\hat{a}_1^\dagger \hat{a}_1 + \hat{a}_2^\dagger \hat{a}_2)^2 \hat{P}_C \propto \hat{P}_C, \quad (\text{D7})$$

which agrees with the numerical results in Sec. E 1, showing an order-of-magnitude improvement for these values of  $\delta$ .

The second term in Eq. (D2) and Eq. (D4) also satisfy the KL condition for any  $\delta$ :

$$\begin{aligned} \hat{P}_C \frac{(\gamma_1 t + \gamma_2 t)}{2} (\hat{a}_1^\dagger \hat{a}_2 \hat{a}_2^\dagger \hat{a}_1 + \hat{a}_2^\dagger \hat{a}_1 \hat{a}_1^\dagger \hat{a}_2) \sin^2 \delta \cos^2 \delta \hat{P}_C \propto \hat{P}_C, \\ \hat{P}_C \hat{M}_0^{(1)} \hat{M}_0^{(2)} \hat{P}_C \propto \hat{P}_C. \end{aligned} \quad (\text{D8})$$

However, the third term in Eq. (D2) fails to satisfy the KL condition for any  $\phi$ :

$$\hat{P}_C((\hat{a}_1^\dagger \hat{a}_2)^2 e^{-2i\phi} + (\hat{a}_2^\dagger \hat{a}_1)^2 e^{2i\phi}) \hat{P}_C \not\propto \hat{P}_C. \quad (\text{D9})$$

Similarly, for the single-photon exchange terms identifying  $E_1 = \hat{M}_1$  and  $E_2 = \hat{M}_2$ , we see that they violate the KL conditions. Their action on the codewords is

$$\hat{a}_1^\dagger \hat{a}_2 |1_N\rangle = \frac{\sqrt{12}}{\sqrt{2}} |3\rangle \otimes |3\rangle, \quad \hat{a}_1^\dagger \hat{a}_2 |0_N\rangle = \frac{\sqrt{12}}{\sqrt{2}} \frac{1}{\sqrt{6}} (|1\rangle + \sqrt{5}|5\rangle) \otimes |1\rangle, \quad (\text{D10})$$

$$\hat{a}_1 \hat{a}_2^\dagger |1_N\rangle = \frac{\sqrt{12}}{\sqrt{2}} |1\rangle \otimes \frac{1}{\sqrt{6}} (|1\rangle + \sqrt{5}|5\rangle), \quad \hat{a}_1 \hat{a}_2^\dagger |0_N\rangle = \frac{\sqrt{12}}{\sqrt{2}} |3\rangle \otimes |3\rangle. \quad (\text{D11})$$

Hence  $\langle i_N | \hat{M}_2^\dagger \hat{M}_1 | j_N \rangle \neq 0$  for  $i \neq j$ , and exact recovery up to first order is impossible:

$$\hat{P}_C \hat{M}_2^\dagger \hat{M}_1 \hat{P}_C \not\propto \hat{P}_C. \quad (\text{D12})$$

## 2. $K = 2, N = 4$ binomial encoding

For  $K = 2, N = 4$ , the first-order evolution is similar to Eq. (D1), except that  $\hat{M}_0$  includes only the first two terms, since the third term vanishes under modular measurements for  $N \neq 2$ :

$$\begin{aligned} \hat{M}_0 = & \frac{1}{2} \left( \gamma_1 t (\hat{a}_1^\dagger \hat{a}_1 \cos^2 \delta + \hat{a}_2^\dagger \hat{a}_2 \sin^2 \delta)^2 + \gamma_2 t (\hat{a}_2^\dagger \hat{a}_2 \cos^2 \delta + \hat{a}_1^\dagger \hat{a}_1 \sin^2 \delta)^2 \right) \\ & + \frac{1}{2} (\gamma_1 t + \gamma_2 t) (\hat{a}_1^\dagger \hat{a}_2 \hat{a}_2^\dagger \hat{a}_1 + \hat{a}_2^\dagger \hat{a}_1 \hat{a}_1^\dagger \hat{a}_2) \sin^2 \delta \cos^2 \delta. \end{aligned} \quad (\text{D13})$$

**Knill–Laflamme conditions:** As shown in Eqs. (D7) and (D8), the no-jump terms satisfy the KL conditions for  $\delta = \pi/4, 3\pi/4$ . Unlike the  $N = 2$  case, the single-photon exchange terms also satisfy the KL conditions, with syndrome measurements  $l = 1, m = 3$  and  $l = 3, m = 1$ . Their action on the codewords is

$$\hat{a}_1^\dagger \hat{a}_2 |1_N\rangle = \frac{\sqrt{40}}{\sqrt{2}} |5\rangle \otimes |7\rangle, \quad \hat{a}_1^\dagger \hat{a}_2 |0_N\rangle = \frac{\sqrt{40}}{\sqrt{2}} \frac{1}{\sqrt{10}} (|1\rangle + \sqrt{9}|9\rangle) \otimes |3\rangle, \quad (\text{D14})$$

$$\hat{a}_1 \hat{a}_2^\dagger |1_N\rangle = \frac{\sqrt{40}}{\sqrt{2}} |3\rangle \otimes \frac{1}{\sqrt{10}} (|1\rangle + \sqrt{9}|9\rangle), \quad \hat{a}_1 \hat{a}_2^\dagger |0_N\rangle = \frac{\sqrt{40}}{\sqrt{2}} |7\rangle \otimes |5\rangle. \quad (\text{D15})$$

Thus  $\langle i_N | \hat{M}_2^\dagger \hat{M}_1 | j_N \rangle = 0$  for  $i \neq j$ , projecting back to the codespace and satisfying the KL condition:

$$\hat{P}_C \hat{M}_2^\dagger \hat{M}_1 \hat{P}_C \propto \hat{P}_C. \quad (\text{D16})$$

**Recovery map:** The no-jump term is corrected using

$$\hat{U}_{00} = \exp\left([\hat{M}_0, \hat{P}_C]\right), \quad (\text{D17})$$

followed by projective measurements

$$\{\hat{P}_L := \hat{P}_C + \hat{P}'_1, \hat{P}_E := (|4\rangle |E\rangle)(\langle 4| \langle E|) + (|E\rangle |4\rangle)(\langle E| \langle 4|) + \hat{P}'_2\}, \quad (\text{D18})$$

where  $\hat{P}'_i$  are complementary projectors ensuring  $\hat{P}_L + \hat{P}_E = \mathbb{I}$ . For the outcome  $\hat{P}_E$ , the unitary correction is

$$\hat{U} = |1_N\rangle \langle 4| \langle E| + |0_N\rangle \langle E| \langle 4| + \hat{U}_{\text{comp.}} \quad (\text{D19})$$

In other words, for this case, after the modular measurement there is an additional measurement, which conditions the unitary to apply. These types of additional measurements in the context of state recovery procedures are also discussed for single-mode binomial codes in Ref.[15].

Single-photon exchange errors are corrected using

$$\hat{U}_{13} = |1_N\rangle\langle 5| + |0_N\rangle\langle 7| + \frac{1}{\sqrt{10}}(|1\rangle + \sqrt{9}\langle 9|)\otimes\langle 3| + \hat{U}_{13}^{\text{comp.}}, \quad (\text{D20})$$

$$\hat{U}_{31} = |1_N\rangle\langle 3| + \frac{1}{\sqrt{10}}(|1\rangle + \sqrt{9}\langle 9|) + |0_N\rangle\langle 7| + \hat{U}_{31}^{\text{comp.}}. \quad (\text{D21})$$

The full Kraus representation of the recovery map is therefore obtained as

$$\tilde{\mathcal{R}} \sim \left\{ \hat{P}_C \hat{U}_{00} (\hat{P}_0 \otimes \hat{P}_0), \hat{U} \hat{P}_E \hat{U}_{00} (\hat{P}_0 \otimes \hat{P}_0), \hat{U}_{13} (\hat{P}_1 \otimes \hat{P}_3), \hat{U}_{31} (\hat{P}_3 \otimes \hat{P}_1) \right\} \cup \{(\hat{P}_l \otimes \hat{P}_m) \mid \text{all other } (l, m)\}. \quad (\text{D22})$$

**Verification of recovery map:** The no-jump correction gives

$$\begin{aligned} & \hat{P}_C (\hat{U}_{00} (\hat{P}_0 \otimes \hat{P}_0) \tilde{\mathcal{N}}(\hat{\rho}) (\hat{P}_0 \otimes \hat{P}_0) \hat{U}_{00}^\dagger) \hat{P}_C \\ & + \hat{U} \hat{P}_E (\hat{U}_{00} (\hat{P}_0 \otimes \hat{P}_0) \tilde{\mathcal{N}}(\hat{\rho}) (\hat{P}_0 \otimes \hat{P}_0) \hat{U}_{00}^\dagger) \hat{P}_E \hat{U}^\dagger \\ & = \hat{\rho} - 10(\gamma_1 t + \gamma_2 t) \hat{\rho} + \mathcal{O}((\gamma_i t)^2), \end{aligned} \quad (\text{D23})$$

where we have used

$$\hat{U}_{00} (\hat{P}_0 \otimes \hat{P}_0) \tilde{\mathcal{N}}(\hat{\rho}) (\hat{P}_0 \otimes \hat{P}_0) \hat{U}_{00}^\dagger = \hat{\rho} - 30(\gamma_1 t + \gamma_2 t) \hat{\rho} + \frac{1}{4}(\gamma_1 t + \gamma_2 t) (\hat{a}_1^\dagger \hat{a}_1 + \hat{a}_2^\dagger \hat{a}_2) \hat{\rho} (\hat{a}_1^\dagger \hat{a}_1 + \hat{a}_2^\dagger \hat{a}_2) + \mathcal{O}((\gamma_i t)^2). \quad (\text{D24})$$

The single-photon exchange correction gives

$$\begin{aligned} & \hat{U}_{13} (\hat{P}_1 \otimes \hat{P}_3) \tilde{\mathcal{N}}(\hat{\rho}) (\hat{P}_1 \otimes \hat{P}_3) \hat{U}_{13}^\dagger \\ & + \hat{U}_{31} (\hat{P}_3 \otimes \hat{P}_1) \tilde{\mathcal{N}}(\hat{\rho}) (\hat{P}_3 \otimes \hat{P}_1) \hat{U}_{31}^\dagger = 10(\gamma_1 t + \gamma_2 t) \hat{\rho} + \mathcal{O}((\gamma_i t)^2). \end{aligned} \quad (\text{D25})$$

Combining these contributions, we recover the initial state up to first order:

$$\tilde{\mathcal{R}} \circ \tilde{\mathcal{N}}(\hat{\rho}) = \hat{\rho} + \mathcal{O}((\gamma_i t)^2). \quad (\text{D26})$$

## Appendix E: Phase measurements and KL conditions at arbitrary dephasing strength for two-mode RSB codes

In Appendix D, we have analysed the effect of Gaussian dephasing channel in its countable Kraus representation, Eq.(B7) and found possible recovery up to the first order. We have shown that an exact recovery map for  $K = 2, N = 4$  two-mode code up to the first order can be found if the encoding mode is fixed to be  $\delta = \pi/4, 3\pi/4$  (independently on  $\phi$ ). In this section, we look at the full Gaussian dephasing channel on two modes in terms of its continuous Kraus operators [13], check under which conditions the KL conditions are satisfied, and study the distinguishability of the codewords under phase measurements.

### 1. Knill-Laflamme matrix for dual codewords under dephasing noise

The effective noisy channel is given by  $\tilde{\mathcal{N}} = \hat{U}_{BS}^\dagger \mathcal{N} \hat{U}_{BS}$  where the noise channel  $\mathcal{N}$  can be expanded in terms of the elements of the continuous Kraus operators,

$$\mathcal{N} \sim \{ \exp(i\hat{A}(\theta_1, \theta_2)) = e^{i\theta_1 \hat{a}_1^\dagger \hat{a}_1 + i\theta_2 \hat{a}_2^\dagger \hat{a}_2} \mid \theta_1, \theta_2 \in [0, 2\pi) \}. \quad (\text{E1})$$

For the effective channel  $\tilde{\mathcal{N}}$ , the transformed Kraus operators take the form:

$$\begin{aligned} \tilde{\hat{A}}(\theta_1, \theta_2) &= \hat{U}_{BS}^\dagger (\theta_1 \hat{a}_1^\dagger \hat{a}_1 + \theta_2 \hat{a}_2^\dagger \hat{a}_2) \hat{U}_{BS} \\ &= \hat{a}_1^\dagger \hat{a}_1 (\theta_1 \cos^2 \delta + \theta_2 \sin^2 \delta) + \hat{a}_2^\dagger \hat{a}_2 (\theta_2 \cos^2 \delta + \theta_1 \sin^2 \delta) \\ &+ (\theta_1 - \theta_2) (e^{-i\phi} \hat{a}_1^\dagger \hat{a}_2 + e^{i\phi} \hat{a}_2^\dagger \hat{a}_1) \sin \delta \cos \delta. \end{aligned} \quad (\text{E2})$$

We analyse the effect of this dephasing channel to find further justifications from the phase measurement perspective for the improvement observed with encoding in a rotated mode, given by  $\delta = \pi/4, 3\pi/4$  and  $\phi = \pi/(2N)$  for a general order- $N$  two-mode RSB code.

It is worth noting that the countable Kraus operators for the dephasing channel,  $\{(\hat{a}^\dagger \hat{a})^l | l \in \mathbb{N}\}$  [13, 23], can be expanded in terms of the continuous Kraus operators shown above are nothing but the rotation operators in the phase space, which allows us to have an intuitive understanding of the *distortion* of information in bosonic systems under dephasing channels. In fact, the dephasing noise can be thought of as diffusion between the probability distributions of the phase measurement outcomes corresponding to the dual codewords. If we choose the encoding mode to be given by  $\delta = \pi/4$ , we obtain

$$\hat{A}(\theta_1, \theta_2) = \frac{1}{2} (\hat{a}_1^\dagger \hat{a}_1 + \hat{a}_2^\dagger \hat{a}_2) (\theta_1 + \theta_2) + \frac{1}{2} (\theta_1 - \theta_2) (e^{-i\phi} \hat{a}_1^\dagger \hat{a}_2 + e^{i\phi} \hat{a}_2^\dagger \hat{a}_1) \quad (\text{E3})$$

$$= \frac{1}{2} (\hat{n}_1 + \hat{n}_2) (\theta_1 + \theta_2) + \frac{1}{2} (\theta_1 - \theta_2) (\hat{G}_{12}^+ \cos \phi - \hat{G}_{12}^- \sin \phi). \quad (\text{E4})$$

Since  $[(\hat{n}_1 + \hat{n}_2), \hat{G}_{12}^\pm] = 0$ , the noise operator  $\exp(i\hat{A}(\theta_1, \theta_2))$  decomposes as

$$\exp\left(\frac{i}{2} (\theta_1 - \theta_2) (\hat{G}_{12}^+ \cos \phi - \hat{G}_{12}^- \sin \phi)\right) \exp\left(\frac{i}{2} (\hat{n}_1 + \hat{n}_2) (\theta_1 + \theta_2)\right). \quad (\text{E5})$$

The off-diagonal entries of the Knill-Laflamme matrix in the dual bases for the two error operators with angles  $(\theta'_1, \theta'_2)$  and  $(\theta''_1, \theta''_2)$  can be now simplified using Eq. (E5) as

$$\langle -_N | \exp(-i\hat{A}(\theta'_1, \theta'_2)) \exp(i\hat{A}(\theta''_1, \theta''_2)) | +_N \rangle = \langle -_N | \exp(i\hat{A}(\theta_1, \theta_2)) | +_N \rangle \quad (\text{E6})$$

where  $\theta_i = \theta''_i - \theta'_i$ . Simplifying this further, we obtain

$$\begin{aligned} & \langle -_N | \exp\left(\frac{i}{2} (\theta_1 - \theta_2) (\hat{G}_{12}^+ \cos \phi - \hat{G}_{12}^- \sin \phi)\right) \exp\left(\frac{i}{2} (\hat{n}_1 + \hat{n}_2) (\theta_1 + \theta_2)\right) | +_N \rangle \\ &= \langle -_N | e^{-i\frac{\pi}{2} \hat{G}_{12}^-} e^{i\frac{\pi}{2} \hat{G}_{12}^+} \exp\left(\frac{i}{2} (\theta_1 - \theta_2) (\hat{G}_{12}^+ \cos \phi - \hat{G}_{12}^- \sin \phi)\right) \exp\left(\frac{i}{2} (\hat{n}_1 + \hat{n}_2) (\theta_1 + \theta_2)\right) e^{-i\frac{\pi}{2} \hat{G}_{12}^-} e^{i\frac{\pi}{2} \hat{G}_{12}^+} | +_N \rangle. \end{aligned}$$

We further see that when  $\phi = 0$ ,

$$\begin{aligned} & \langle -_N | \exp\left(\frac{i}{2} (\theta_1 - \theta_2) \hat{G}_{12}^+\right) \exp\left(\frac{i}{2} (\hat{n}_1 + \hat{n}_2) (\theta_1 + \theta_2)\right) | +_N \rangle \\ &= - \langle -_N | \exp\left(-\frac{i}{2} (\theta_1 - \theta_2) \hat{G}_{12}^+\right) \exp\left(\frac{i}{2} (\hat{n}_1 + \hat{n}_2) (\theta_1 + \theta_2)\right) | +_N \rangle \\ &= - \langle -_N | e^{-i\pi \hat{n}_2} e^{i\pi \hat{n}_2} \exp\left(-\frac{i}{2} (\theta_1 - \theta_2) \hat{G}_{12}^+\right) \exp\left(\frac{i}{2} (\hat{n}_1 + \hat{n}_2) (\theta_1 + \theta_2)\right) e^{-i\pi \hat{n}_2} e^{i\pi \hat{n}_2} | +_N \rangle \\ &= - \langle -_N | \exp\left(\frac{i}{2} (\theta_1 - \theta_2) \hat{G}_{12}^+\right) \exp\left(\frac{i}{2} (\hat{n}_1 + \hat{n}_2) (\theta_1 + \theta_2)\right) | +_N \rangle. \end{aligned} \quad (\text{E7})$$

Here we have used the fact that  $e^{i\frac{\pi}{2} \hat{G}_{12}^-}$  acts as the logical  $X$  operator on the codespace and  $N$  is an even number. We have also used the commutator relation  $[\hat{G}_{12}^-, \hat{G}_{12}^+] = 2i(\hat{a}_1^\dagger \hat{a}_1 - \hat{a}_2^\dagger \hat{a}_2)$ . Thus from the above equality in Eq.(E7), we can conclude

$$\langle -_N | \exp\left(\frac{i}{2} (\theta_1 - \theta_2) \hat{G}_{12}^+\right) \exp\left(\frac{i}{2} (\hat{n}_1 + \hat{n}_2) (\theta_1 + \theta_2)\right) | +_N \rangle = 0. \quad (\text{E8})$$

For the existence of exact recovery, we further require that the diagonal entries are equal. However for this channel, we see

that they differ as shown below:

$$\begin{aligned}
& \langle +_N | \exp\left(\frac{i}{2}(\theta_1 - \theta_2)(\hat{G}_{12}^+ \cos \phi - \hat{G}_{12}^- \sin \phi)\right) \exp\left(\frac{i}{2}(\hat{n}_1 + \hat{n}_2)(\theta_1 + \theta_2)\right) |+_N \rangle \\
&= \langle -_N | e^{-i\frac{\pi}{N}\hat{n}_2} \exp\left(\frac{i}{2}(\theta_1 - \theta_2)(\hat{G}_{12}^+ \cos \phi - \hat{G}_{12}^- \sin \phi)\right) \exp\left(\frac{i}{2}(\hat{n}_1 + \hat{n}_2)(\theta_1 + \theta_2)\right) e^{i\frac{\pi}{N}\hat{n}_2} |-_N \rangle \\
&= \langle -_N | \exp\left(\frac{i}{2}(\theta_1 - \theta_2)\left(\hat{G}_{12}^+ \cos\left(\frac{\pi}{N} - \phi\right) + \hat{G}_{12}^- \sin\left(\frac{\pi}{N} - \phi\right)\right)\right) \exp\left(\frac{i}{2}(\hat{n}_1 + \hat{n}_2)(\theta_1 + \theta_2)\right) |-_N \rangle, \quad (\text{E9})
\end{aligned}$$

where we have used the relations  $e^{-i\frac{\pi}{N}\hat{n}_2} \hat{G}_{12}^\pm e^{i\frac{\pi}{N}\hat{n}_2} = \hat{G}_{12}^\pm \cos \frac{\pi}{N} \pm \hat{G}_{12}^\mp \sin \frac{\pi}{N}$  for the proof. However, from the above expression in Eq.(E9), we see that the two diagonal entries can be brought arbitrarily close to each other by setting  $\phi = (2m + 1)\frac{\pi}{2N}$  for  $m \in \mathbb{Z}$ , and taking the limit  $N \rightarrow \infty$ . Moreover, we also see that for all  $\theta_1 = \theta_2$  corresponding to the case of correlated dephasing, the entries given in Eq.(E9) are exactly equal. This justifies the existence of the recovery circuit in Fig. 3. Note that the above discussion holds for any of the general two-mode instantiations of our codes, namely given by Eqs.(4) and (5), and in particular for any even rotation symmetry order  $N$ .

We exemplify this analytical understanding with numerical calculation of the entanglement infidelity for the case of the  $N = 2, K = 2$  two-mode codes. As shown in Fig.5, the infidelity is minimized for the optimal encoding angles,  $\delta = \pi/4, 3\pi/4$  and  $\phi = \pi/4$ . We have also numerically checked that for  $N = 4, K = 2$ , the infidelity is minimized for the optimal encoding angles,  $\delta = \pi/4, 3\pi/4$  and  $\phi = \pi/8$ .

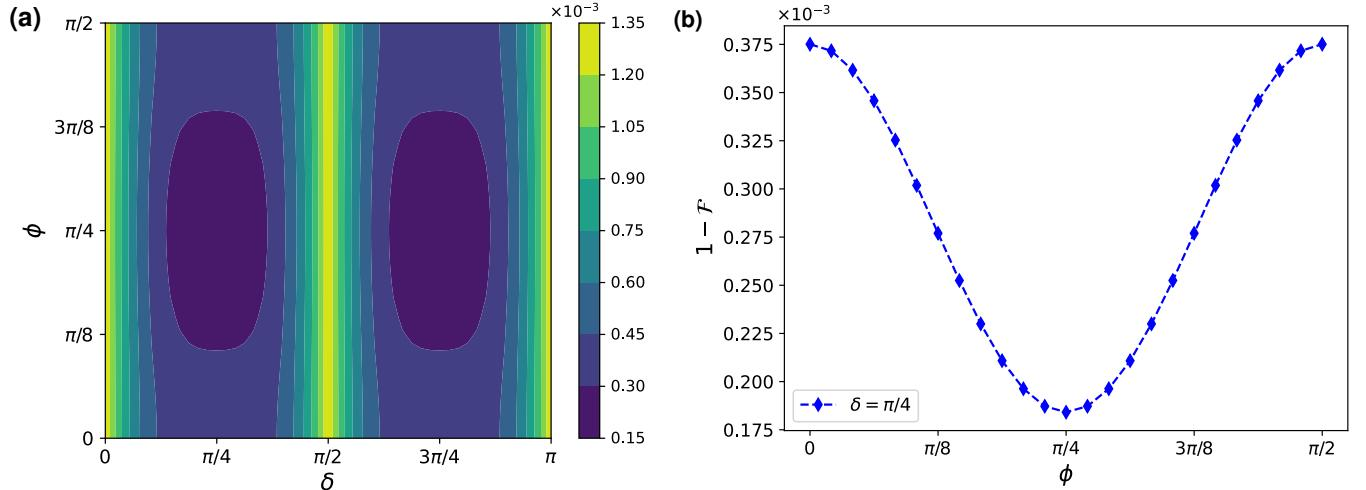


FIG. 5: (a) Entanglement infidelity as a function of  $\delta$  and  $\phi$ , showing minima for  $\delta = \pi/4, 3\pi/4$  for  $N = 2, K = 2$  against dephasing  $\gamma_1 t = \gamma_2 t = 10^{-3}$ . (b) The variation of entanglement infidelity as a function of  $\phi$  is very small (of the order  $10^{-3}$ ). We however still observe that the lowest value is obtained from  $\phi = \pi/4$  which is  $\pi/(2N)$  for  $N = 2$  and  $m = 0$ .

## 2. Distinguishing the dual codewords and understanding the phase trajectories

In this Section, we will see how the two-mode code is distinct in performance under dephasing as compared to a single mode code in terms of the phase distinguishability of the codewords. Similar to the case of single-mode RSB, the dual codewords,  $|\pm_N\rangle$  encoded in the two-mode RSB, are related by a rotation in either mode, up to a global phase:  $\exp\left(i\frac{\pi}{N}\hat{a}_2^\dagger\hat{a}_2\right)|\pm_N\rangle = |\mp_N\rangle$ ;  $\exp\left(i\frac{\pi}{N}\hat{a}_1^\dagger\hat{a}_1\right)|\pm_N\rangle = -|\mp_N\rangle$ .

The *joint phase measurement* in each of the modes formally can be written as a set of *positive operator-valued measures* (POVM):  $\{\hat{\Pi}(\phi_1) \otimes \hat{\Pi}(\phi_2) \mid \phi_1, \phi_2 \in [0, 2\pi]\}$ , where  $\hat{\Pi}(\phi)$  is defined e.g. in Ref.[28]. The outcomes of such measurement is  $(\phi_1, \phi_2)$ . In the absence of any noise, outcomes  $(0, \pi/N) \bmod (2\pi/N)$  or  $(\pi/N, 0) \bmod (2\pi/N)$  indicate that the logical state is  $|-_N\rangle$ , while the measurement outcomes  $(0, 0) \bmod (2\pi/N)$  or  $(\pi/N, \pi/N) \bmod (2\pi/N)$  indicate that the logical state is  $|+_N\rangle$  (Fig. 6).

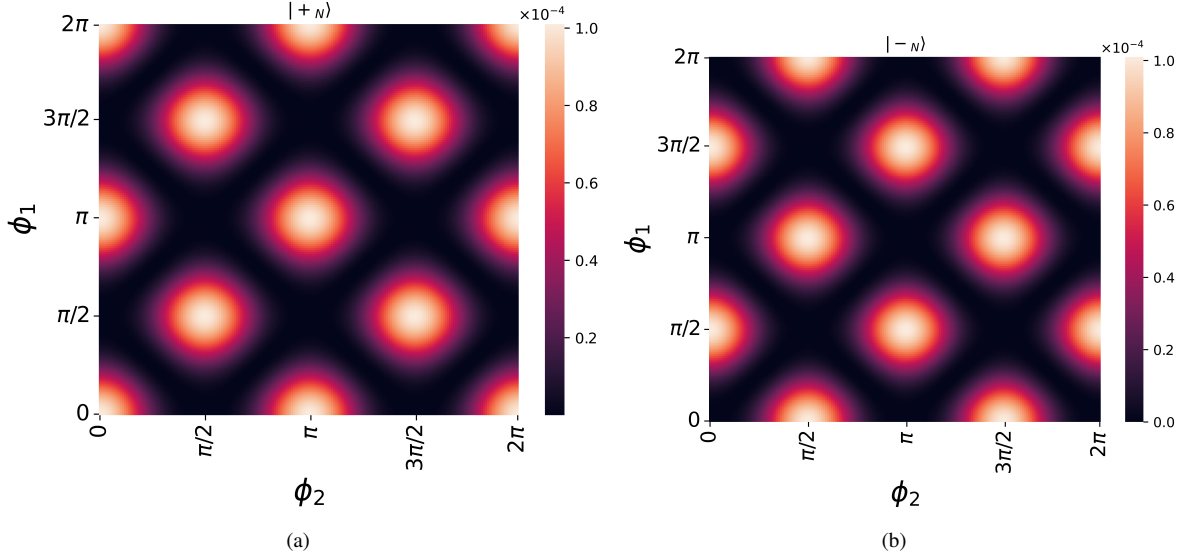


FIG. 6: Probability distribution of phase measurement outcome for the dual basis encoded in  $K = 2, N = 2$  two-mode code.

As we have previously found out, for  $\delta = 0$  in Eq. (E2), the physical error operators,  $\exp(i\hat{A}(0, \pi/N))$  and  $\exp(i\hat{A}(\pi/N, 0))$  acts as logical  $Z$  operator. Hence, in this case, the probability distribution outcome of the joint phase measurement can be used to distinguish the codewords for *small enough* rotation errors only, parametrised by  $\theta_1, \theta_2 \ll \pi/N$ . This allows us to distinguish the dual codewords with high accuracy for small enough errors.

However for large rotation errors, for example  $(\pi/N, 0), (0, \pi/N)$ , the joint probability distribution for the dual codewords maps into one another, as these errors act as logical  $Z$  operator.

On the other hand, if we consider the case,  $\delta = \pi/4$ , from Eq. (E2) we have

$$\hat{A}(\theta_1, \theta_2) = \frac{1}{2} (\hat{a}_1^\dagger \hat{a}_1 + \hat{a}_2^\dagger \hat{a}_2) (\theta_1 + \theta_2) + \frac{1}{2} (\theta_1 - \theta_2) (e^{-i\phi} \hat{a}_1^\dagger \hat{a}_2 + e^{i\phi} \hat{a}_2^\dagger \hat{a}_1) \quad (\text{E10})$$

$$= \frac{1}{2} (\hat{n}_1 + \hat{n}_2) (\theta_1 + \theta_2) + \frac{1}{2} (\theta_1 - \theta_2) (\hat{G}_+ \cos \phi - \hat{G}_- \sin \phi). \quad (\text{E11})$$

As we know that  $[(\hat{n}_1 + \hat{n}_2), \hat{G}_\pm] = 0$ , the noise operators decomposes as

$$\hat{A}(\theta_1, \theta_2) = \exp\left(\frac{i}{2}(\theta_1 - \theta_2)(\hat{G}_+ \cos \phi - \hat{G}_- \sin \phi)\right) \exp\left(\frac{i}{2}(\hat{n}_1 + \hat{n}_2)(\theta_1 + \theta_2)\right). \quad (\text{E12})$$

As shown in Appendix E, and in particular in Eq.(E8), for  $\delta = \pi/4$  and  $\phi = 0$ , the overlap between the codewords as it evolves under the dephasing Kraus operators, remains zero:

$$\langle -N | \exp(i\hat{A}(\theta_1, \theta_2)) | +N \rangle = 0 \quad \forall \theta_1, \theta_2. \quad (\text{E13})$$

This is in stark contrast with the single-mode and  $\delta = 0$  two-mode cases, where the overlap can be non-zero. Moreover, if we look at the joint probability distribution of phase measurement outcomes of the dual codewords as shown in Fig. 7, we find that their support are largely mutually exclusive for all rotation errors. This allows us to distinguish the dual codewords with high accuracy, even for large rotation errors. However we re-emphasise that exact error-correction is generally still not possible since as shown in the previous section, the diagonal entries of the Knill-Lafflame equations are not equal (Eq.(E9)).

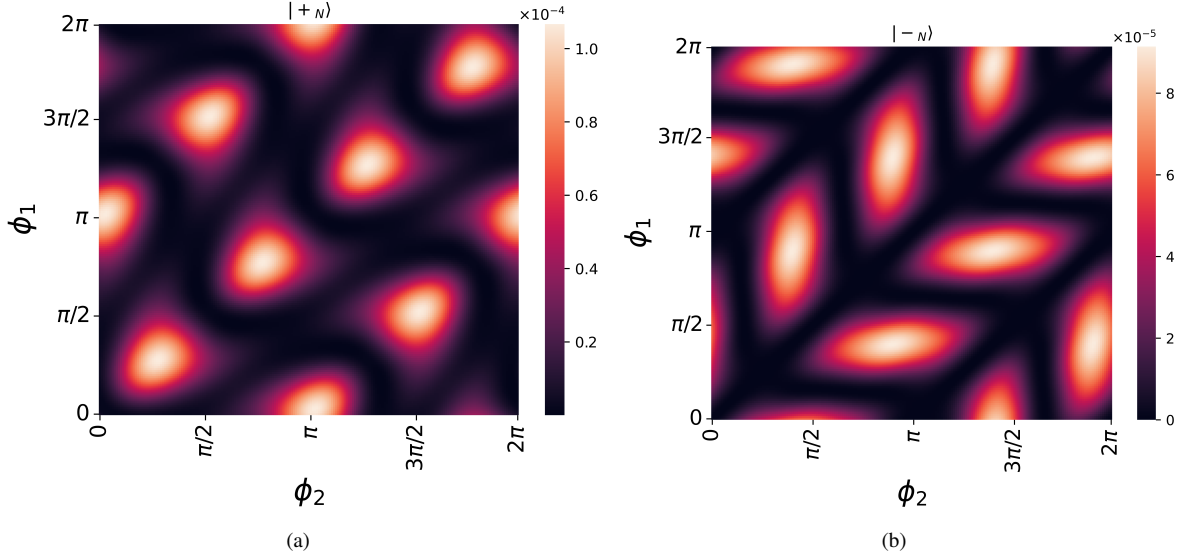


FIG. 7: *Probability distribution of phase measurement outcome for the dual basis encoded in  $K = 2, N = 2$  two-mode code under a rotation  $\exp(i\hat{A}(0.2\pi, 0))$  for the encoding axis given by  $\delta = \frac{\pi}{4}, \phi = 0$ .*

It should also be noted that Eq. (E13) holds true for Gaussian dephasing alone, and does not imply that the evolution of trace distance between the codewords under an arbitrary dephasing channel is always unity. In general, the noisy codewords are not perfectly distinguishable for an arbitrary dephasing channel. A future work may explore whether such non-overlapping distribution of the outcomes of phase measurements can be used to design an error-correcting circuit similar to the teleportation circuit due to Knill [13, 42]. Finally, also note that as the energy of the binomial codes (parameterised by  $K$  for binomial codes) increases, the probability distribution of the outcomes for the dual codewords has vanishing overlap [13], suggesting a better performance against the dephasing noise can be found with increasing  $K$  (while with losses a sweet-spot in average energy is to be expected).

#### Appendix F: Performance of two-mode rotation symmetric bosonic codes under the influence of random telegraph noise

Here we present numerical results on the performance of simple instances of our two-mode binomial code ( $K = 2, N = 2$ ), for different choices of the encoding angles, against Random Telegraph Noise.  $\xi$  is the switching rate and  $\nu$  is the amplitude of the RTN. We refer to Ref.[28] for a thorough definition of the noise, along with the parameters. The plot in Fig.8 shows that the optimal encoding angles yield an increased performance against RTN noise, and that such performance beats the case of the corresponding single-mode binomial code.

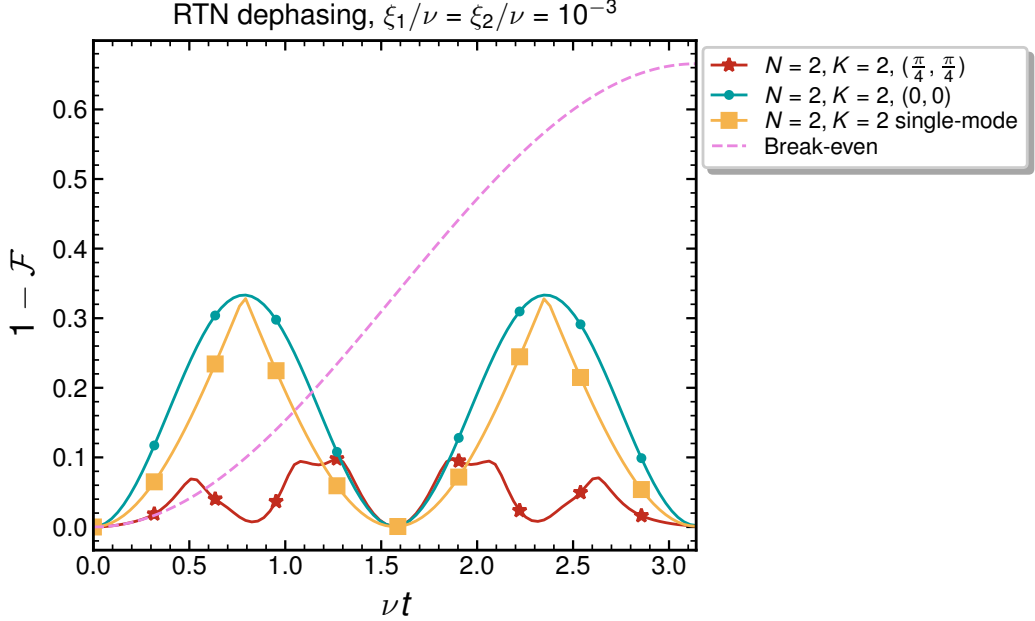


FIG. 8: A comparison between the optimal performance of the single-mode binomial code,  $K = 2, N = 2$  and the simplest instance of the two-mode order- $N$  RSB code,  $K = 2, N = 2$  inner binomial concatenated with outer dual rail. Specifically we investigate the performance of the code, upon a beam-splitting action with angle  $(\pi/4, \pi/4)$  after the preparation of the logical state in the modes  $\hat{a}_1, \hat{a}_2$ .

#### Appendix G: Exact recovery circuit for correlated dephasing

Here we show that correlated dephasing can be corrected perfectly, and we derive the corresponding recovery map. Since the beam-splitting operation  $\hat{U}_{BS}$  commutes with the Kraus operators of correlated dephasing, i.e.,  $[(\hat{n}_1 + \hat{n}_2), U_{BS}(\delta, \phi)] = 0$  for each  $\delta, \phi$ , the analysis holds independently of the choice of encoding angles.

First, we observe that the action of the controlled operation

$$CX_{NL} = \exp\left(i \frac{\pi}{2N} \hat{n}_1 \otimes \hat{G}_{34}^-\right)$$

on the four-mode Fock states appearing in the tensor product of two codewords of the form in Eqs. (4) and (5) gives

$$\begin{aligned} CX_{NL} |2mN, (2n+1)N\rangle \otimes |2pL, (2q+1)L\rangle &= |2mN, (2n+1)N\rangle \otimes e^{i\pi m \hat{G}_{34}^-} |2pL, (2q+1)L\rangle \\ &= |2mN, (2n+1)N\rangle |2pL, (2q+1)L\rangle \end{aligned} \quad (G1)$$

$$\begin{aligned} CX_{NL} |2mN, (2n+1)N\rangle \otimes |(2q+1)L, 2pL\rangle &= |2mN, (2n+1)N\rangle \otimes e^{i\pi m \hat{G}_{34}^-} |(2q+1)L, 2pL\rangle \\ &= |2mN, (2n+1)N\rangle |(2q+1)L, 2pL\rangle \end{aligned} \quad (G2)$$

$$\begin{aligned} CX_{NL} |(2n+1)N, 2mN\rangle \otimes |2pL, (2q+1)L\rangle &= |(2n+1)N, 2mN\rangle \otimes e^{i\frac{\pi}{2}(2n+1) \hat{G}_{34}^-} |2pL, (2q+1)L\rangle \\ &= |(2n+1)N, 2mN\rangle |(2q+1)L, 2pL\rangle \end{aligned} \quad (G3)$$

$$\begin{aligned} CX_{NL} |(2n+1)N, 2mN\rangle \otimes |(2q+1)L, 2pL\rangle &= |(2n+1)N, 2mN\rangle \otimes e^{i\frac{\pi}{2}(2n+1) \hat{G}_{34}^-} |(2q+1)L, 2pL\rangle \\ &= |(2n+1)N, 2mN\rangle |(2pL, (2q+1)L)\rangle. \end{aligned} \quad (G4)$$

Summing over the indices  $m, n, p$ , and  $q$  in the above expressions, one finds that  $CX_{NL} |0\rangle_N \otimes |a\rangle_L = |0\rangle_N \otimes |a\rangle_L$  and  $CX_{NL} |1\rangle_N \otimes |a\rangle_L = |1\rangle_N \otimes |a \oplus a\rangle_L$ , indicating that it acts as a controlled- $X$  gate on the codespace of the two-mode codes.

Using these expressions, the map corresponding to the circuit in Fig. 3, with  $CX_{LN} = \exp\left(i \frac{\pi}{2N} \hat{n}_3 \otimes \hat{G}_{21}^-\right)$ , is given by

$$\begin{aligned}
& \mathcal{R}(\mathcal{N}(\hat{\rho}) \otimes |0\rangle\langle 0|_L) \\
&= CX_{LN} CX_{NL} (\mathcal{N}(\hat{\rho}) \otimes |0\rangle\langle 0|_L) CX_{NL}^\dagger CX_{LN}^\dagger \\
&= \sum_{a,b=0,1} \rho_{ab} CX_{LN} CX_{NL} \left( \int_{-\infty}^{\infty} d\phi p_t(\phi) e^{i\phi(\hat{n}_1 + \hat{n}_2)} |a\rangle\langle b|_N e^{-i\phi(\hat{n}_1 + \hat{n}_2)} \otimes |0\rangle\langle 0|_L \right) CX_{NL}^\dagger CX_{LN}^\dagger \\
&= \sum_{a,b=0,1} \rho_{ab} \left( \int_{-\infty}^{\infty} d\phi p_t(\phi) e^{i\phi(\hat{n}_1 + \hat{n}_2)} CX_{LN} |a\rangle\langle b|_N \otimes |a\rangle\langle b|_L CX_{LN}^\dagger e^{-i\phi(\hat{n}_1 + \hat{n}_2)} \right). \tag{G5}
\end{aligned}$$

Here we have used the fact that the  $CX$  gate commutes with the correlated dephasing operator, since  $[(\hat{n}_i + \hat{n}_j), \hat{G}_{ij}^-] = 0$ , and that the controlled- $X$  operation satisfies  $CX_{NL} |a\rangle_N |0\rangle_L = |a\rangle_N |a\rangle_L$ .

For a given  $a$  and  $b$ , we further find that

$$\begin{aligned}
& CX_{LN} |a\rangle_N \otimes |a\rangle_L \langle b|_N \otimes \langle b|_L CX_{LN}^\dagger \\
&= |(a \oplus a)\rangle_N \otimes |a\rangle_L \langle (b \oplus b)|_N \otimes \langle b|_L \\
&= |0\rangle\langle 0|_N \otimes |a\rangle\langle b|_L. \tag{G6}
\end{aligned}$$

Substituting this into Eq. (G5), we obtain

$$\begin{aligned}
\mathcal{R}(\mathcal{N}(\hat{\rho}) \otimes |0\rangle\langle 0|_L) &= \left( \int_{-\infty}^{\infty} d\phi p_t(\vec{\phi}) e^{i\phi(\hat{n}_1 + \hat{n}_2)} |0\rangle\langle 0|_N e^{-i\phi(\hat{n}_1 + \hat{n}_2)} \right) \otimes \sum_{a,b=0,1} \rho_{ab} |a\rangle\langle b|_L \\
&= \mathcal{N}(|0\rangle\langle 0|_N) \otimes \sum_{a,b=0,1} \rho_{ab} |a\rangle\langle b|_L. \tag{G7}
\end{aligned}$$

This holds for an arbitrary choice of the two-mode codewords in Eqs. (4) and (5), not only for the case of binomial codes.

## Appendix H: Hadamard gate and $T$ gate

In this Appendix, we include the circuits that implement the Hadamard and  $T$  gates via gate teleportation. The schemes are direct extensions of those proposed for single-mode RSB codes [13] to the two-mode setting (see Fig. 9). We first show how the controlled rotation ( $CROT$ ) gate acts as a logical controlled- $Z$  ( $CZ$ ) gate on our encoded two-mode codespace.

The  $CROT$  gate is defined as

$$CROT_{NL} = \exp\left(\frac{i\pi}{NL} \hat{n}_1 \otimes \hat{n}_3\right),$$

where  $\hat{n}_1$  and  $\hat{n}_3$  are the photon number operators associated with the first modes of the control and target rails, respectively. The gate acts on the four-mode Fock states appearing in the tensor product of two codewords as

$$\begin{aligned}
CROT_{NL} |2mN, (2n+1)N\rangle \otimes |2pL, (2q+1)L\rangle &= e^{i\pi 2m2p} |2mN, (2n+1)N\rangle \otimes |2pL, (2q+1)L\rangle \\
&= |2mN, (2n+1)N\rangle |2pL, (2q+1)L\rangle \tag{H1}
\end{aligned}$$

$$\begin{aligned}
CROT_{NL} |2mN, (2n+1)N\rangle \otimes |(2q+1)L, 2pL\rangle &= e^{i\pi 2m2(q+1)} |2mN, (2n+1)N\rangle \otimes |(2q+1)L, 2pL\rangle \\
&= |2mN, (2n+1)N\rangle |(2q+1)L, 2pL\rangle \tag{H2}
\end{aligned}$$

$$\begin{aligned}
CROT_{NL} |(2n+1)N, 2mN\rangle \otimes |2pL, (2q+1)L\rangle &= e^{i\pi(2n+1)2p} |(2n+1)N, 2mN\rangle \otimes |2pL, (2q+1)L\rangle \\
&= |(2n+1)N, 2mN\rangle |2pL, (2q+1)L\rangle \tag{H3}
\end{aligned}$$

$$\begin{aligned}
CROT_{NL} |(2n+1)N, 2mN\rangle \otimes |(2q+1)L, 2pL\rangle &= e^{i\pi(2n+1)(2q+1)} |(2n+1)N, 2mN\rangle \otimes |(2q+1)L, 2pL\rangle \\
&= - |(2n+1)N, 2mN\rangle |(2q+1)L, 2pL\rangle. \tag{H4}
\end{aligned}$$

Summing over the indices, one can verify that  $CROT_{NL}$  acts as a controlled- $Z$  gate on the logical codespace  $\{|a_N\rangle \otimes$

$$|b_L\rangle, a, b \in \{0, 1\}.$$

To illustrate the Hadamard-gate protocol in Fig. 9 (a), we first prepare an auxiliary two-mode encoded qubit in the state  $|+_M\rangle = \frac{1}{\sqrt{2}}(|0_M\rangle + |1_M\rangle)$  and entangle it with the state  $|\psi_N\rangle = \alpha|0_N\rangle + \beta|1_N\rangle$  to be teleported:

$$CROT|\psi_N\rangle \otimes |+_M\rangle = \alpha|0_N\rangle|+_M\rangle + \beta|1_N\rangle|-_M\rangle. \quad (\text{H5})$$

Rewriting the order- $N$  state in the  $\pm$  basis and the order- $M$  state in the computational basis, we obtain

$$CROT|\psi_N\rangle \otimes |+_M\rangle = \frac{\alpha}{2}(|+_N\rangle + |-_N\rangle) \otimes (|0_M\rangle + |1_M\rangle) + \frac{\beta}{2}(|+_N\rangle - |-_N\rangle) \otimes (|0_M\rangle - |1_M\rangle). \quad (\text{H6})$$

Measuring the first (control) rail in the  $\pm$  basis yields the output state on the target rail as  $\alpha|+_M\rangle + \beta|-_M\rangle$  for the outcome “+” and  $\alpha|+_M\rangle - \beta|-_M\rangle$  for the outcome “-”. Combining both cases, with  $i = 0$  for “+” and  $i = 1$  for “-”, the output state is

$$\bar{X}^i \bar{H} |\psi_M\rangle, \quad (\text{H7})$$

where  $\bar{H}$  acts as the logical Hadamard gate on the two-mode codespace.

The same reasoning applies for the  $T$ -gate circuit in Fig. 9 (b). Writing  $|T_M\rangle = \frac{1}{\sqrt{2}}(|0_M\rangle + e^{\frac{i\pi}{4}}|1_M\rangle)$ , one obtains the logical  $\bar{T}$  or  $\bar{T}\bar{X}$  gate depending on whether the measurement outcome is “+” or “-”, respectively.

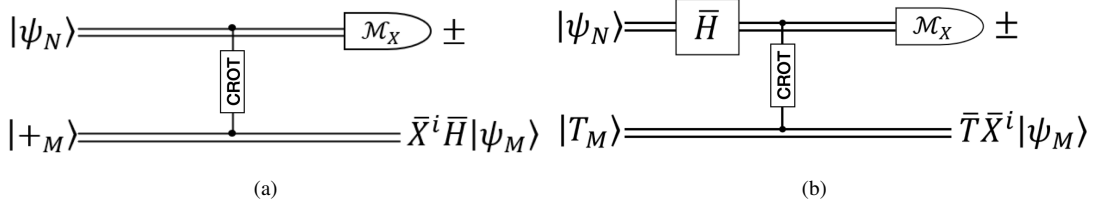


FIG. 9: Implementation of the (a) Hadamard gate and (b)  $T$ -gate for the two-mode rotation-symmetric codes using gate teleportation.